SENSORS

Neuro-inspired electronic skin for robots

Fengyuan Liu[1]†, Sweety Deswal[1]†, Adamos Christou[1], Yulia Sandamirskaya[2], Mohsen Kaboli[3,4], Ravinder Dahiya[1]*

Copyright © 2022 The Authors, some rights reserved; exclusive licensee American Association for the Advancement of Science. No claim to original U.S. Government Work

Touch is a complex sensing modality owing to large number of receptors (mechano, thermal, pain) nonuniformly embedded in the soft skin all over the body. These receptors can gather and encode the large tactile data, allowing us to feel and perceive the real world. This efficient somatosensation far outperforms the touch-sensing capability of most of the state-of-the-art robots today and suggests the need for neural-like hardware for electronic skin (e-skin). This could be attained through either innovative schemes for developing distributed electronics or repurposing the neuromorphic circuits developed for other sensory modalities such as vision and audio. This Review highlights the hardware implementations of various computational building blocks for e-skin and the ways they can be integrated to potentially realize human skin–like or peripheral nervous system–like functionalities. The neural-like sensing and data processing are discussed along with various algorithms and hardware architectures. The integration of ultrathin neuromorphic chips for local computation and the printed electronics on soft substrate used for the development of e-skin over large areas are expected to advance robotic interaction as well as open new avenues for research in medical instrumentation, wearables, electronics, and neuroprosthetics.

INTRODUCTION

The sense of touch is crucial to cope with the everyday challenges related to interaction with objects, to safely manipulate and explore them to understand their physical properties (*1*), and for perception and self-awareness (*2*). When deprived of reliable tactile information [e.g., through the numbness of anesthetized or cold fingers (*3*, *4*)], people become clumsy, and accidents are prone to occur. Similarly, tactile sensing or haptics also has a vital role in the development of cognitive and intelligent robotic systems because it allows them to autonomously explore their surroundings. Robotic systems of the future thus need touch sensing to safely interact in dynamic, unstructured, and often uncertain environments. As a result, during the past several decades, researchers have explored numerous ways to create an artificial sense of touch through various types of sensors in bendable and stretchable form factors (*5*–*8*) [e.g., resistive (*9*), piezoresistive (*10*, *11*), capacitive (*12*), optical (*13*), piezoelectric (*14*, *15*), acoustic (*16*)]—either individually or as a stack (*17*), and yet, we are far from the tactile sensing capabilities possessed by humans. Some of the key developments for tactile sensing or electronic skin (e-skin) in robotics are shown in Fig. 1.

For a robot to have human-level perceptual capability, it is important to associate the tactile sensors with a similar data processing system in the way that receptors work in the peripheral nervous system (PNS). This requires physically distributed computing hardware on soft substrates, along with tactile sensors. Although tactile sensors have received substantial attention in the past, the data encoding and processing using dedicated hardware has not been explored as much. The tactile information processing in robotics so far has mainly involved analytical or data-driven approaches, using a software platform (*18*). Analytical approaches exploit physics-based models to obtain tactile information, such as object properties and action commands, from the raw tactile data. However, these models often rely on structured interactions and do not provide accurate information needed for control or robust perception. The alternative is to use data-driven methods that learn mappings from raw sensory data, or lower-level features, to high-level object properties and action commands. In this regard, supervised, unsupervised, and reinforcement learning can be explored. Hierarchical representations, such as neural networks, are often used to learn multiple levels of features (*19*, *20*). Flexible representations allow the robot to adapt the learned model to the specific task based directly on data. The analytical, data-driven, or algorithmic approaches can be more effective with distributed computing in tactile skin (*21*). The neural-like hardware developed for other sensory modalities, such as vision and audio, or the chips developed to imitate the working of central nervous system (CNS) (*22*–*24*) can be repurposed for tactile data processing. However, such solutions are not ideal for tactile sensing, because unlike other sensory modalities, tactile sensing is physically distributed all over the body and requires mechanical softness to interact with other objects.

Robotics has considerably advanced from using few sensors in the hands to using large numbers of sensors all over the body (Fig. 1) to meet the requirements of emerging tasks that exploit the large-area or whole-body contact to manipulate objects or navigate through unstructured or cluttered environments. With increasing numbers of sensors, the amount of tactile data they generate can rapidly approach practical limits, such as occupying the communication bandwidth. As such, it is impractical to send all of the data to the robot's centralized computing hardware (an equivalent of the brain). Likewise, the power requirements can be considerably high. This calls for e-skin to have efficient data handling capability, and it could be achieved through distributed low-power electronic hardware for computing. This notion aligns with the way the PNS complements the CNS.

Focusing on the computing hardware for e-skin, this Review complements previous review articles that have presented topics such as various types of tactile sensors (*25*–*28*), techniques, and materials (for example, using liquid metal and hydrogel) to realize sensors in soft and flexible form factors (*29*, *30*), identification of object properties

[1]Bendable Electronics and Sensing Technologies (BEST) Group, James Watt School of Engineering, University of Glasgow, G12 8QQ Glasgow, UK. [2]Neuromorphic Computing Intel Labs, Munich, Germany. [3]Department of Research, New Technologies, Innovation, BMW Group, Parkring 19, 85748 Garching bei Munchen, Germany. [4]Cognitive Robotics and Tactile Intelligence Group, Donders Institute for Brain, Cognition, and Behaviour, Radboud University, Nijmegen, Netherlands.
*Corresponding author. Email: ravinder.dahiya@glasgow.ac.uk
†These authors contributed equally to this work.

Downloaded from https://www.science.org at Huazhong University of Science and Technology on September 02, 2026

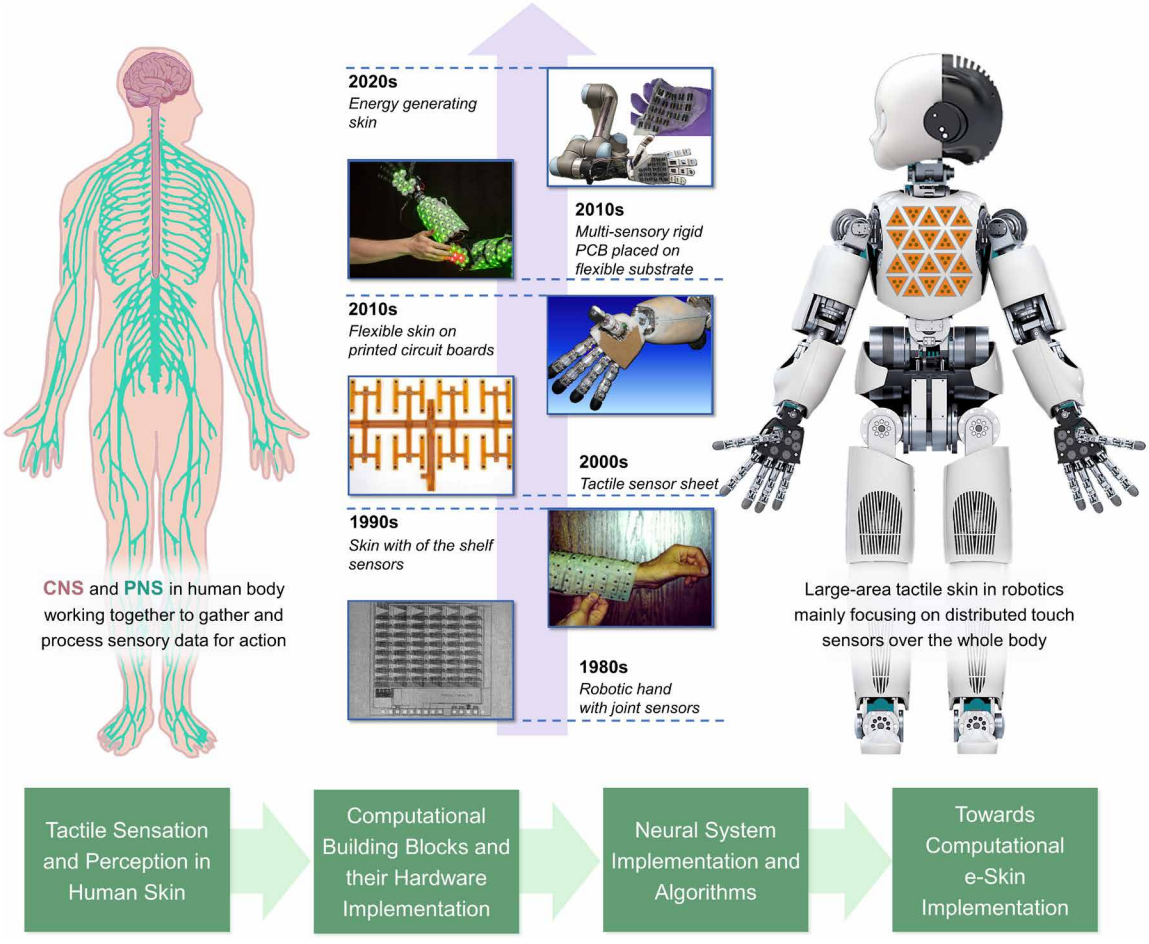


Fig. 1. The tactile sensation and perception in human skin and the evolution of artificial tactile skin in robots. Skin is the major component of human PNS (left), which has inspired robotic tactile skin research over the years. The tactile sensing technologies have advanced from single-touch sensor to large-area skin (middle) covering the whole body of a robot (right). This poses challenges in data handling and energy consumption. The images (from bottom to top) in the timeline (middle) are adapted from (*146*, *147*, *184*–*187*) with permissions. Distributing computing in tactile skin can further boost the interaction capabilities of robots. The block diagram below shows the key steps to attain the same and outlines the structure of this paper. The image of the robot on the right-hand side is an adaptation from the image "iCub Humanoid platform," created by "antoni gràcia." Link of the original image: https://www.behance.net/gallery/17635773/iCub-Humanoid-platform Link for the license: https://creativecommons.org/licenses/by-nc/4.0/legalcode.

and interactions (*31*), and distributed energy (*32*, *33*). This article also complements previous reviews covering neuro-/bio-inspired e-skin (*34*–*36*), providing a systematic and comprehensive discussion on the computing element in tactile sensing. In this regard, this Review is distinct and timely. The discussion starts from a biological perspective, summarizing the state-of-the-art viewpoints related to tactile data encoding and processing in PNS. The discussion also highlights the key message for the hardware implementation of neural-like processing in e-skin. This is followed by the discussion on various building blocks for hardware implementations. Although some of these building blocks are not developed for e-skin, they can be repurposed to develop one to address the challenges stated above. The pathways for the integration of these building blocks with possible algorithms, leading to the development of computational e-skin, are discussed afterward. We then present how the implementation of large-area computational e-skin could gain from the advances in flexible and printed electronics technologies. The intelligent robotic skin capable of extracting low-level information from the abundant tactile data could also open new application avenues in areas such as medical instruments, wearables, and neuroprosthetics, and therefore, researchers working in these diverse areas will benefit from this article.

TACTILE SENSATION AND PERCEPTION IN HUMAN SKIN

Constructing a robust perceptual system for robots based on the tactile sensory information is a critical but challenging task. Because humans manage this almost effortlessly, the human body is an excellent reference to follow. This section presents some fundamental but vital features in the tactile sensation and perception in human body, especially at the PNS level with a view to realizing computational e-skin for the next generation of robots.

The human body acquires the tactile sensory information through thousands of mechanoreceptors distributed over the skin (Table 1), as shown in Fig. 2A. This large number of receptors ensures a reliable sensation but poses challenges in data transmission. The biological solution is to use action potentials, sometimes with adaptation, to encode, communicate, and control the body (*37*). Such a manner is

IMAGE CREDITS: TOP TO BOTTOM FOR TIMELINE (*146*, *147*, *184*–*187*)/IEEE

Downloaded from https://www.science.org at Huazhong University of Science and Technology on September 02, 2026

Table 1. Typical properties of human skin (*78, 194–204*). NA, not available.

Location	Relative area (%) (*78, 194, 203*)	Strain (%) (*196–201*)	No. of mechanoreceptors (*195, 202*)	Spatial acuity (cm)* (*204*)
Finger	~1.3	35–45	~13,350	~0.2
Foot	~6.1	<30†	1,000–5,000	0.8–1.8
Chest	~12.8	<30†	~13,000	~3.2
Back	~13.9	<30†	2,000–14,000	~1.3
Shoulders	~1.9	NA	~4,000	~3
Abdomen	~3.6	NA	~4,000	~3.6
Thigh	~18.3	<30†	~30,000	~2.3
Wrist	~0.7	10–40	~1,500	~4.2
Knee	~1.2	30–40	~2,000	~4.7
Elbow	NA	60	NA	~4.2

*Spatial acuity denotes the two-point discrimination threshold. †Data are anticipated according to the value from other areas of the skin.

highly beneficial in terms of reducing power consumption and data latency.

Reverse engineering to develop the e-skin requires knowledge beyond neuroscience principles. For example, from a structure viewpoint, the skin is soft and present over a large area. With a large number of receptors (of varying thresholds) distributed at different depths, the skin can respond to the stimuli of various frequencies [fast adapting (FA) and slow adapting (SA)] (*38*). Moreover, each subtype of receptors shows a different size of receptive field; they overlap with each other and are interconnected locally (*39–41*). Such an intricate nature forms the foundation of the fine spatial sensitivity of the skin. Toward this, several works have reported various sensors that provide similar functionalities as SA and FA receptors and also suggest their stacking to mimic the mechanoreceptor arrangement in the skin (Fig. 2A) (*17*, *42*, *43*).

Compared with tactile sensation, the understanding of the tactile perception is far less developed. The general view is that the perception starts at the cuneate (second-order tactile) neuron (in the spinal cord), while the first-order neuron (sensory neuron) is solely responsible for the tactile sensing (*38*). However, it is also argued that the mechanical properties such as the softness of skin may also be related to the perception process. Some level of computing takes place in the skin itself owing to the location-specific tactile sensing characteristics inside the receptive field of sensory neuron and the soft nature of the skin, which deforms during contact (Fig. 2B) (*44*, *45*). In this regard, the spiking pattern from the first-order neuron could contain some information of the edge orientation. Although more similar studies are needed to unravel the perceptual element of tactile sensing in biological skin, hardware implementation of some level of computation in the artificial skin will be beneficial. It is because, unlike biosystem where hyperconnectivity is regular, the electronic system usually has a much lower fan-out/fan-in ratio, with one fan-in leading to three to four fan-out on average in digital electronics (*46*). The realization of a hyperconnected electronic system is challenging from both a design and a fabrication perspective. Another reason is that the flexible, stretchable nature of the artificial skin poses a major hurdle to reliable data transmission. The large number of receptors confined in a limited area could markedly increase the difficulty of data transmission without losing fidelity. Instead, achieving edge computing at the skin level itself could greatly lower the data transmission burden. Like the audio and vision, it is also argued that the tactile sensory data are processed via time division: The firing pattern of several neurons at the same time would trigger the firing of the next-level neuron and, in turn, strengthen the afferent synapse (Fig. 2C) (*47*). By doing so, the tactile sensation aroused by an object is correlated with the firing of one (or multiple) second-order neuron(s), and the generated spiking patterns are sent for further processing (Fig. 2C). This lays the foundation for tactile signal computing using the spiking time–dependent plasticity (STDP) learning rule. Nevertheless, this is not the only rule available. Other possible learning rules, whether or not they are biomimetic, can be implemented in the e-skin to enable the intelligent data processing. This is discussed in the "Neural system implementation and algorithms" section.

COMPUTATIONAL BUILDING BLOCKS AND THEIR HARDWARE IMPLEMENTATIONS

To fully mimic the functionality of the biological skin and the associated PNS, the building blocks that can function as sensors, neurons, and synapse are required (Fig. 2A). This section reviews the hardware devices mimicking sensory neurons and cuneate neurons and the synaptic devices needed between these two sets of neurons. The functionalities required from the individual building blocks, along with their preliminary integration in a neural pathway for robotic applications, are discussed in the subsequent subsections.

Artificial neuron

The neuron is the basic processing unit in the biological neural system, where analog incoming signals are integrated and converted into action potentials when the spatiotemporal summation exceeds the firing threshold of the neuron. Previous studies have identified approximately 20 typical spiking features in the biological system, such as tonic spiking, tonic bursting, and phasic spiking (*48*). Among them, some features have been widely observed and play important roles in somatosensation. The capability of delivering such spiking features, for example, frequency adaptation, should be one of the criteria for the hardware implementation of neuron block for the e-skin. Here, we review the state-of-the-art strategies that have been

Downloaded from https://www.science.org at Huazhong University of Science and Technology on September 02, 2026

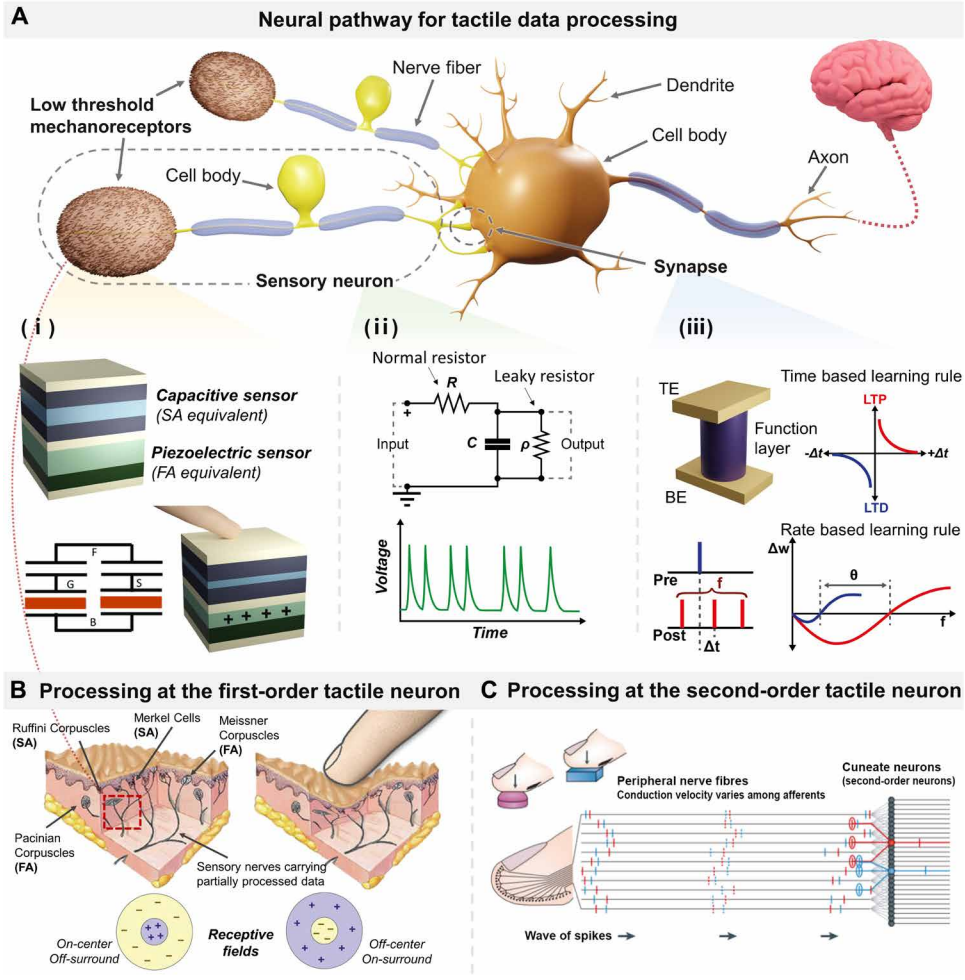


Fig. 2. The neural pathways for tactile data processing in human skin and their simple implementation schemes using basic devices and circuits. (**A**) Neural pathway for tactile data processing. The sensing data are collected in the sensory neuron (first order), passed to the cuneate neuron (second order), and finally sent to the higher levels of the nervous system. The key components (mechanoreceptors, neurons, and synapses) of human body involved in tactile sensing and data encoding are shown with the illustrations of their simple implementations through electronic devices and circuits. The SA and FA mechanoreceptors are usually mimicked by a stack of capacitive and piezoelectric sensors (*17*) (i). The RC circuit (ii) emulates the action potential of the spiking neuron (*63*). Memristors or similar devices (iii) can be used for the implementation of various synaptic functions such as time- and rate-based learning rules. The rate-based learning rule refers to BCM (Bienenstock, Cooper, and Munro) learning rule. (**B**) Possible tactile data processing at the first-order neuron (*44*, *188*). Reprinted with permission from (*188*). (**C**) Possible tactile data processing at the second-order neuron. Reprint from (*47*) with permission.

developed for sensory neuron (that is, neuromorphic sensors) and then the neuron circuits in general, which can be used for the realization of the second-order tactile neuron.

Sensory neuron (neuromorphic sensor)

The sensory neuron is the first-order neuron in the tactile neural pathway. The sensors designed for the computational e-skin should output the spiking signal, and to this end, the two hardware implementation approaches have been explored so far. One is to integrate the sensor with oscillating and edge-detection circuits, as illustrated in Fig. 3A (*49*–*52*), and the second is to interface the sensor with the neuron circuits, as shown in Fig. 3B (*53*, *54*). Both approaches could provide biological features such as spiking rate dependency (class 1 excitable) and event-driven sensing. However, the shape of the spiking signal they generate is different. Because the first strategy uses an AND gate, it generates square-shaped spikes (Fig. 3A); in contrast, the conventional neuron circuits using Si complementary metal-oxide semiconductor (CMOS) can deliver biologically plausible spiking patterns including the hyperpolarization and depolarization stages, refractory period (Fig. 3B). Because the shape of the spike governs the plasticity-based learning of artificial synapses, the synaptic devices need to be identified and designed carefully along with the associated neurons. From the engineering point of view, the first strategy relies on the digital circuit and can be more robust to disturbance. In this regard, some parts have been successfully demonstrated on flexible substrates using printing techniques. However, considering the whole neural system, the simplified spiking signal generated by the oscillating circuits cannot offer some of the vital spiking features observed in biology. To realize a system with rich neural dynamics, the second strategy may be required.

Considering the open and unpredictable environment the skin typically experiences, the sensors need to exhibit excellent specificity/selectivity, particularly because the e-skin requires multimodal sensing to detect various parameters such as stress, pressure, and temperature. This can be challenging because the electronic systems themselves are temperature sensitive. Nevertheless, there are many encouraging works showing excellent specificity regardless of ambient variations (*55*–*59*). Alternatively, one could use low-specificity sensors and calibrate later, for example, at the second-order neuron stage.

Cuneate neuron

This subsection discusses the strategies for the hardware implementation of spiking neuron and their evaluation in terms of the biological plausibility, that is, the number of the biologically observed spiking features, and the implementation cost measured by the active devices required in the design. The neuron circuit discussed here can be used to realize the second-order tactile neuron for the computational e-skin. From the model point of view, several mathematical equations have been proposed to describe the neuron spiking process. These include leaky integrate-and-fire model (*60*), Hodgkin-Huxley (*61*), and Izhikevich model (*62*). These neuron models can be implemented using one or two capacitors with leaky resistors to emulate the important features observed in biological neurons (*63*) (Fig. 2A), such as spatiotemporal integration

Downloaded from https://www.science.org at Huazhong University of Science and Technology on September 02, 2026

IMAGE CREDITS: (B) (*188*)/IEEE (C) (*47*)/SPRINGER NATURE

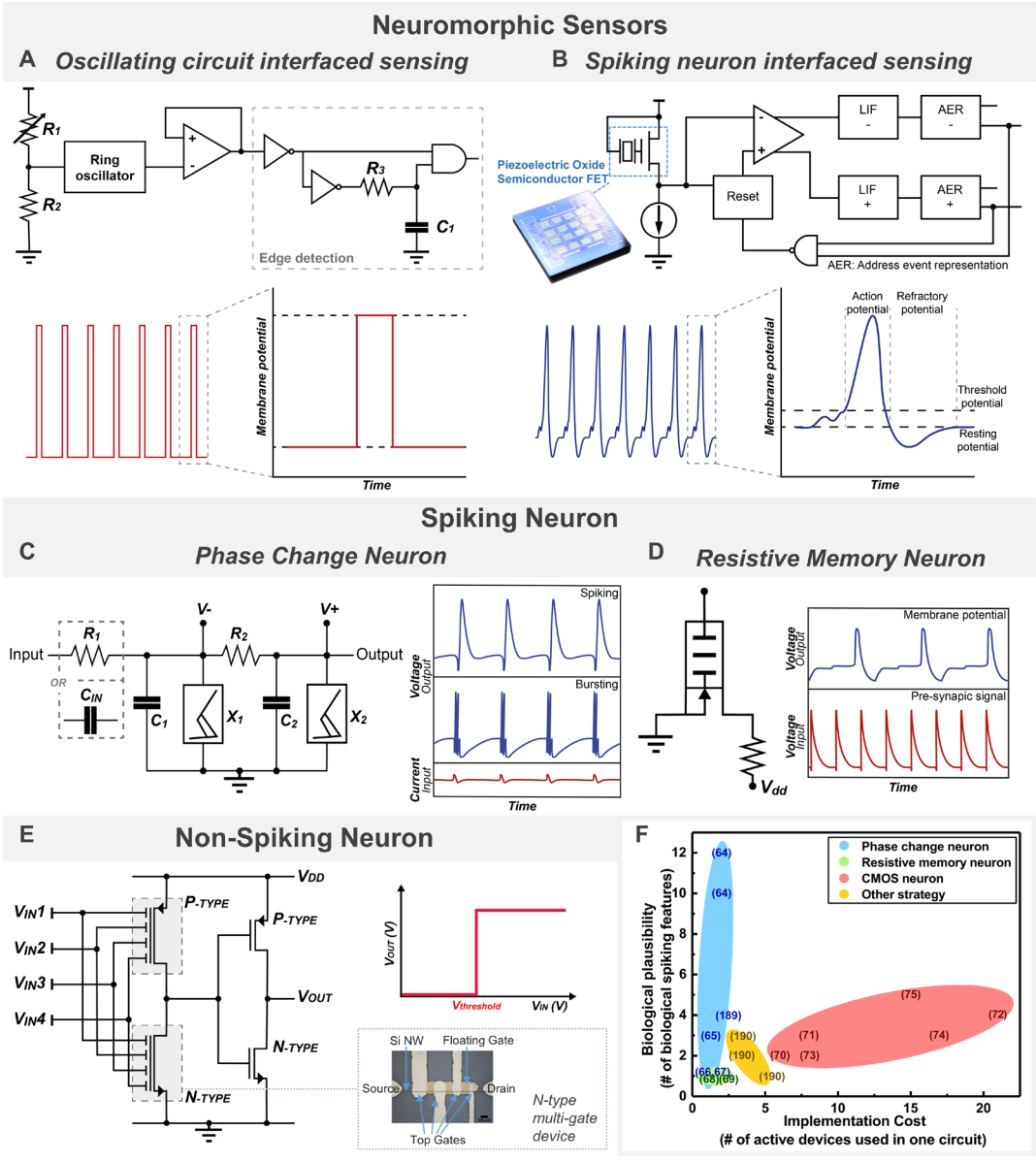


Fig. 3. The hardware implementation of an artificial neuron. (**A**) and (**B**) show the strategies to develop a neuromorphic sensor. (A) An oscillating circuit–based neuromorphic sensor. This strategy uses digital circuits and thus is easier for the hardware implementation on soft substrates as demonstrated in (*49*–*52*). (B) A neural circuit–based neuromorphic sensor (*53*). Such a strategy is able to provide a more biomimetic spiking signal. However, it is still a challenge for the hardware implementation in soft platforms, especially over large areas. (**C**) and (**D**) show the strategies to develop spiking neuron circuit in general. (C) The phase-change device–based spiking neuron (*64*). (D) The volatile resistive memory–based spiking neuron (*69*). (**E**) The strategy to implement the nonspiking neuron using a multigate transistor. Adapted from (*78*). (**F**) The performance comparison of various spiking neurons, with data extracted from (*64*–*75*, *189*, *190*). The criteria of the biological plausibility are based on the spiking patterns discussed in (*48*). As can be seen from the figure, the neuron circuits based on novel materials/devices require a smaller number of active devices compared with the CMOS-based neurons.

and all-or-none rule. In this regard, the components showing a leaky resistance are the key to the hardware implementation of neuron circuits.

One way to emulate the leaky component is to use phase-change devices (Fig. 3C). The resistance of such a device remains high under a low voltage bias, owing to an insulating phase, and shows an abrupt transition to a low resistance state (metallic phase) when sufficiently high bias voltage is available. Such a transition is reversible depending on the voltage bias. A highly biomimetic neuron circuit can be realized with only two leaky phase-change devices: Each controls a capacitor, thus mimicking the neuron's opening and closing of the sodium and potassium channels gated by voltage. Such a design can emulate almost all the spiking features found in biological neurons—including tonic and phasic spiking, tonic and phasic bursting, and frequency adaptation (Fig. 3C) (*64*)—and thus can be used to realize a neural system with rich neural dynamics. It is also possible to implement a neuron circuit with only one phase-change device (*65*–*67*), although in this case the spiking signal generated cannot fully mimic the

Downloaded from https://www.science.org at Huazhong University of Science and Technology on September 02, 2026

biological spiking features. Overall, the phase-change device–based design offers the lowest hardware complexity (Fig. 3F).

The leaky resistive device can also be realized with volatile resistive memristors (*68*, *69*), whose resistance switching is governed by the voltage bias across the device (Fig. 3D). From a fabrication viewpoint, it seems relatively easier to fabricate the resistive memristors, and thus, they may hold more promise for the large-area implementations on soft substrates.

A more common strategy is to use CMOS circuits (*70*–*75*). In this case, the subthreshold behavior of metal-oxide semiconductor field-effect transistor (MOSFET) is used to emulate the resistance change. Unlike phase-change and memristive devices, the MOSFETs are three-terminal devices whose channel resistance is controlled by the gate voltage. The CMOS neuron requires a complicated layout to control the resistance of the MOSFETs channel, to mimic the leaky behavior. The comparison between the hardware complexity and the biological plausibility for each strategy has been illustrated in Fig. 3F.

The spiking-based computing system consumes substantially less power. For example, the energy required for the neuron circuit based on phase-change device can be as low as 100 fJ per spike (*76*). This value can be even lower for CMOS neurons (~4 fJ) (*71*). Assuming a moderate firing rate of 100 Hz, the energy required per neuron per second is in the order of picojoule. For a direct comparison, we use the power consumption of Intel Core i7-920 microprocessor as a reference. This microprocessor consumes a power of 85 W with 731 million transistors. This corresponds to ~100-nJ energy consumption per second for a single transistor or several hundreds of nanojoules for a single gate—this is substantially higher than the power consumption of a neuron circuit.

Nonspiking neuron

The nonspiking neuron is another alternative where a continuous function represents the firing rate and thus presents a simplified activation function. Both digital and analog circuits have been explored for implementation of nonspiking functionalities, although they usually have a complex layout and consume high power. Attempts have been made to seek alternatives such as on VO_2-based Mott devices (*77*) and nanowire-based neural FETs (*78*) to achieve rectified linear unit and threshold function, respectively (Fig. 3E). The benefits of using a nonspiking neuron include easy and highly accurate training of the associated neural network. However, their relatively higher power requirements compared with the spiking neuron are a major drawback. Thus, the selection of spiking or nonspiking neurons as the building block for the computational e-skin may vary with the application.

Artificial synapse

As the core building block of a neural network, the synapse has two main functionalities: the synaptic efficacy (the ability to pass the signal) and the synaptic plasticity (the ability to adapt the weight according to various learning rules). To replicate such functionalities in hardware, CMOS circuits and novel electronic devices (*79*–*83*) have been explored, for both artificial neural network (ANN) and spiking neural network (SNN).

For the proposed computational e-skin, the hardware implementation over large areas with flexible/stretchable substrates is desired, and the incompatibility of CMOS devices with soft and conformable materials raises some challenges. Alternatives such as memristive devices on flexible substrates have been explored to realize compact artificial synapse. A variety of organic and inorganic materials have been explored to develop resistive random access memory (RRAM) (*84*, *85*), phase-change memory (PCM) (*86*–*88*), magnetic random access memory (MRAM) (*89*), and ferroelectric random access memory (FeRAM) (*90*), leading to two- and three-terminal structures. Such devices exploit the change in physical properties of the material in response to external electrical stimuli to mimic the general synaptic behavior (Fig. 4A). The memristive crossbar arrays (*91*) are a concise and attractive route for implementation of synapses (Fig. 4B). For ANN, the operation of synapse is usually achieved by using a single pulse signal, with the aim to achieve a long retention time with multilevel weight tuning (Fig. 4C). Contrary to ANN, the SNN is more biologically plausible because it operates the synaptic devices using a pair of pulses (pre- and post-) after various biological learning rules, for example, STDP (Fig. 2A) (*92*–*96*). Figure 4D illustrates some examples of hardware-implemented large-scale artificial synapses: They are in the rigid form factor. The future development of large-scale synapses for e-skin should be carried out on soft substrates.

Although crossbar arrays provide a concise architecture, they could lead to several potential problems as well. For example, the sneak path issue (current leakage through unselected cells) is a well-known bottleneck for the large-area implementation of memristive crossbar arrays. In addition, the requirement of electrical forming process for each memristor pixel could enhance the hardware complexity, which may make the filamentary memristive devices less suitable for the large-area implementation. Selector devices such as transistor (*97*) or self-selective (passive) memristive crossbar (*98*) have been investigated to overcome the sneak path issues. Recently, a passive crossbar array was directly implemented with CMOS circuit allowing online learning and vector matrix multiplications, thus providing operational neuromorphic computing hardware (*99*). The hardware implementation of high-performance, high-yield, and uniform one transistor–one memristor (1T1M) crossbar arrays for convolutional neural networks is another example of energy-efficient large-scale networks (*100*). Using transistors as selector devices leads to 1T1M structure (*101*), which may be used for synaptic functionality in e-skin. However, their large form factor needs to be considered as well. To this end, one solution is to merge the selector device with RRAM (*102*, *103*), which allows a higher lateral and vertical integration than the conventional 1T1M configuration.

Despite several reports on RRAM-based artificial synapses, their hardware realization is limited possibly because of challenges such as poor resistance tuning, spatial and temporal variability, device yield, and nonlinearity/asymmetry. These issues negatively affect the performance of neuromorphic computing (*104*). On the other hand, the floating gate transistors offering better uniformity are actively being explored for synaptic functionalities (*105*–*108*), which are considered as a more mature technology due to their compatibility with CMOS fabrication process. Emerging synaptic transistors with various working mechanisms like electrochemical (*109*), charge trapping/detrapping (*110*), and light assistive reaction (*111*, *112*) have also been reported along with their application in neuromorphic tactile sensing and processing system (*113*, *114*). Some hardware implementations of these devices are worthwhile; however, efforts are needed to achieve the response uniformity over a large area, with desired retention and endurance (*115*). As mentioned above, for robotic skin, the flexibility/stretchability of artificial synapse is critical, and in this regard, the soft synaptic transistors (*116*–*118*) and memristors (*119*, *120*) are relevant. Flexible high-performance synaptic transistors have been reported to mimic the native biological synapses. Likewise, on the basis of

Downloaded from https://www.science.org at Huazhong University of Science and Technology on September 02, 2026

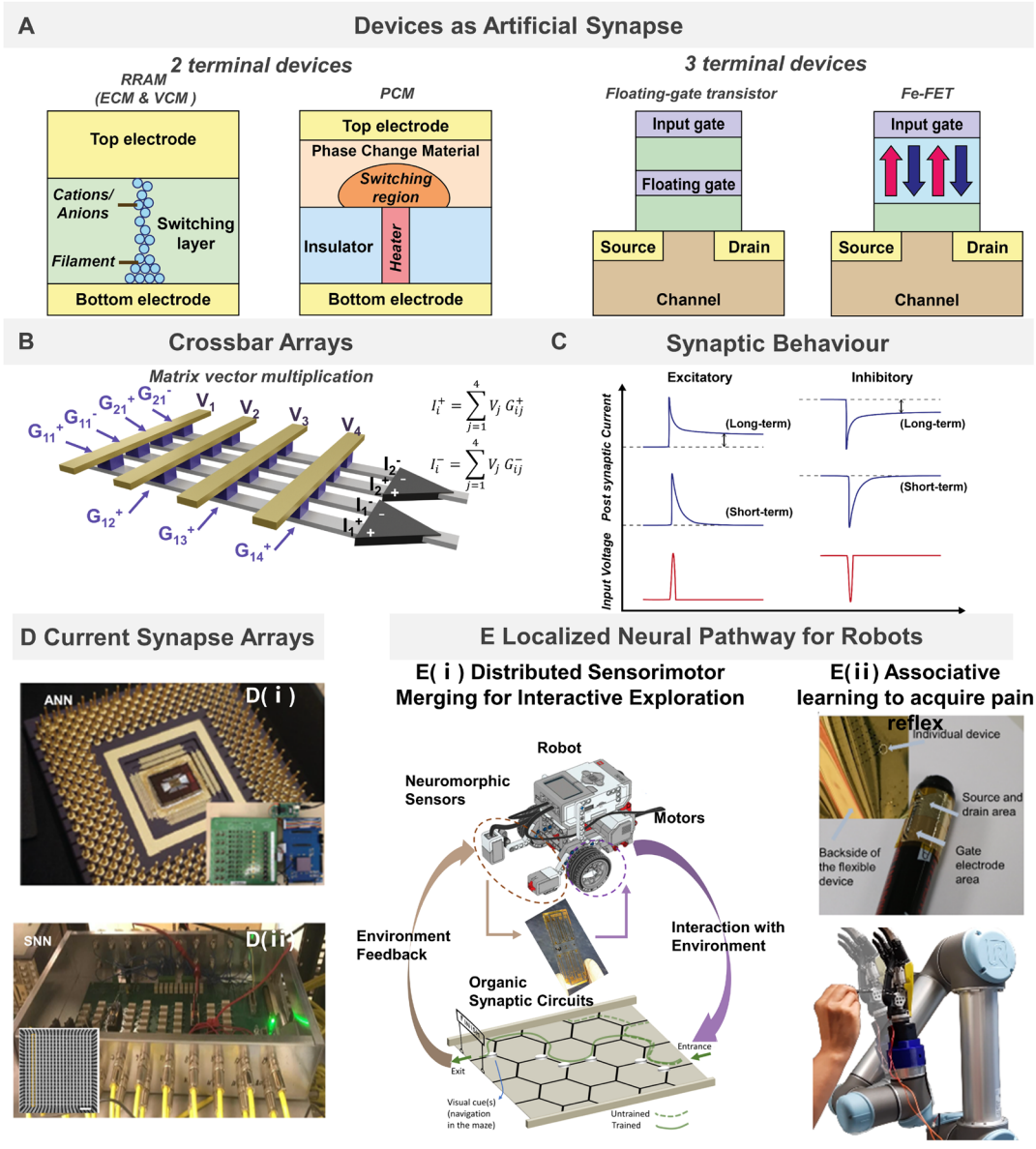


Fig. 4. Hardware Implementation of artificial synapse. (**A**) Various two- and three-terminal devices as artificial synapses including RRAM, PCM, floating gate transistor, and Fe-FET. The schemas of the RRAM, PCM, and floating-gate transistor are redrawn based on (*191*). (**B**) Matrix vector multiplication in crossbar arrays with both active and passive memristive devices. Potentiation and depression characteristics of analog memristive devices. (**C**) Synaptic behavior as excitatory and inhibitory with long- and short-term plasticity. (**D**) Hardware implementation of some memristor-based artificial synapse in (i) ANN [reprint from (*99*) with permission. Copyright 2019, Springer Nature] with integration of memristor crossbars and CMOS chips on wire-bonded pin-grid array package (inset shows the testing setup) and (ii) SNN [reprint from (*95*) with permission] using PCB with passive memristor switching matrix (inset shows the scanning electron image of memristor crossbar). (**E**) Localized neural pathway for robots. (i) Distributed sensorimotor merging that leads to the learning of the maze exploration of the robot. Adapted from (*127*) with permission. (ii) Distributed sensorimotor correlation that leads to the acquisition of the pain reflex. Reprint from (*128*) with permission.

IMAGE CREDITS: (A) (*191*)/SPRINGER NATURE (D) (i) (*99*); (ii) (*95*)/SPRINGER NATURE

flexible memristors, a three-dimensional (3D) artificial synaptic network has been reported to enable direct correlated learning and trainable memory capability (*121*). A new class of flexible memristors based on 2D materials (*122*) is also very attractive, with compatibility of solution processing and printing technology. The thickness of 2D materials in subnanometer range further facilitates low operating voltages and switching speed (*115*), but it is still lacking in terms of large-area scalability and uniformity. Recent reports on flexible (*121*) and stretchable (*118*, *123*) artificial synapses are encouraging because these devices are suitable for large-area robotic skin.

The performance of an artificial synaptic device is typically assessed in terms of multilevel states, linearity, retention, endurance, dynamic range, variability, device area, device yield, and energy consumption. However, not all of these device metrics are critical to every application, and they can depend on the training algorithm

Downloaded from https://www.science.org at Huazhong University of Science and Technology on September 02, 2026

and specific task. A comparison of some of the hardware-implemented synaptic devices is demonstrated in Table 2. The technology for such novel neuromorphic devices is at an infancy, and despite their advantages, now, they are unable to replace CMOS technology at the commercial hardware level. A hybrid design, for example, memristor-based analog computing along with CMOS-based digital computing, maybe the solution in the near future.

Peripheral neural pathway for robots

Robots require sensory-motor fusion and adaptive interaction with the environment. Specifically, skin-like tactile sensing has been used in robotics for tactile-based environmental exploration, physical human-robot interaction and collaboration, objects' physical properties recognition, tool manipulation, and locomotion (*18*, *124*, *125*). However, most of these demonstrations are achieved by software approaches in a centralized computing unit, that is, the equivalent of brain. In addition, these platforms usually use digital circuitries, which add to the latency of the process. Instead, in organisms, localized sensory-motor coordination and integration has been widely observed (*126*). Such a decentralized, analog processing notably reduces the data latency for robots. For this, the building blocks discussed above can be used to construct the localized computing platform needed for tactile sensing, opening avenues for next-generation robots (Fig. 4E).

For example, the agent-environment interaction is required for the exploration and learning of robots. As shown in Fig. 4E (i), reinforcement learning could be done in a localized manner using distributed synaptic circuits to learn the maze exploration by the robots (*127*). Similarly, robots need to work in unknown environments with the potential to sense the impending hazard. This can be achieved by the correlation between the sensory and motor signal, allowing the robot to identify the pain signal and respond to it (*128*). Owing to the use of the synaptic device [Fig. 4E (ii)], the withdrawal reflex behavior could be mimicked in a concise manner. The above examples show how decentralized computing can be constructed in a simple neural configuration, benefiting the next-generation robots. In the next section, possible neural network structures are discussed, which could potentially be used for carrying out more complicated tasks for robots.

NEURAL SYSTEM IMPLEMENTATION AND ALGORITHMS

The neural network structure

This section presents the possible neural system structure for the computational e-skin along with its training algorithms. This includes one layer of sensory neurons and one layer of cuneate neurons, connected via synapses (Fig. 5A). As discussed in the "Tactile sensation and perception in human skin" section, the subtypes of mechanoreceptors have different sizes of receptive fields, which overlap and are interconnected to form the basis for the spatial sensitivity of the skin (*40*, *129*). We present a similar concept for the proposed neural network (Fig. 5A). The stimulation of one neuron could influence other neighboring neurons, and thus, it is possible to map the incoming tactile signal to a higher-dimensional space in the first layer; the output is fed into the second layer for further processing. The proposed neural network is similar to the reservoir computing. However, owing to soft tissues, the native skin is more complex: The receptive fields of the neighboring mechanoreceptors are modulated by the external tactile stimuli (Fig. 2B) (*130*, *131*). This is one of the unique aspects of tactile sensing (*44*), and mimicking the same could be a future direction of e-skin research. The proposed neural network is capable of carrying out various tasks required by robots, such as local tactile feature recognition and contact/slippage detection. Nevertheless, it is also necessary to consider what kinds of tasks are suitable for localized processing at the skin level. One possible direction is that a higher-level arrangement can be made in a similar manner to organisms in nature. For example, as discussed in earlier, differentiating the edge orientation of a tactile stimulus is a task processed in the skin level for humans (*45*), and similar tactile perception could be realized with the computational e-skin as well.

The learning algorithms

Implementing the proposed neural network using the hardware building blocks is another important aspect to consider. Various learning strategies including supervised, unsupervised, and reinforcement learning are available. However, developing an all-hardware–based supervised learning system can be costly in terms of devices or circuits needed (*97*, *132*, *133*) and will thus not be discussed for the e-skin. On the other hand, the plasticity-based learning rule, STDP, is the fundamental learning rule in SNNs and leads to unsupervised

Table 2. Hardware-integrated artificial synapse devices.

Reference	Memristive device configuration	Cell dimension (μ m^2)	Size of crossbar array	Energy consumption	Application of hardware system
(*205*)	1M	10 × 10	15 × 6	0.31 μJ	Recognition of printed digits
(*100*)	1T1M	0.5 × 0.5	128 × 16	371.89 pJ	MNIST (National Institute of Standards and Technology) image recognition
(*206*)	1M	<0.5 × 0.5	32 × 32	719.0 μJ	Pattern matching and natural image processing
(*99*)	1M	0.5 × 0.5	54 × 108	1.12 pJ	Demonstration of different computing models
(*95*)	1M	–	20 × 20	–	Coincidence detection

Downloaded from https://www.science.org at Huazhong University of Science and Technology on September 02, 2026

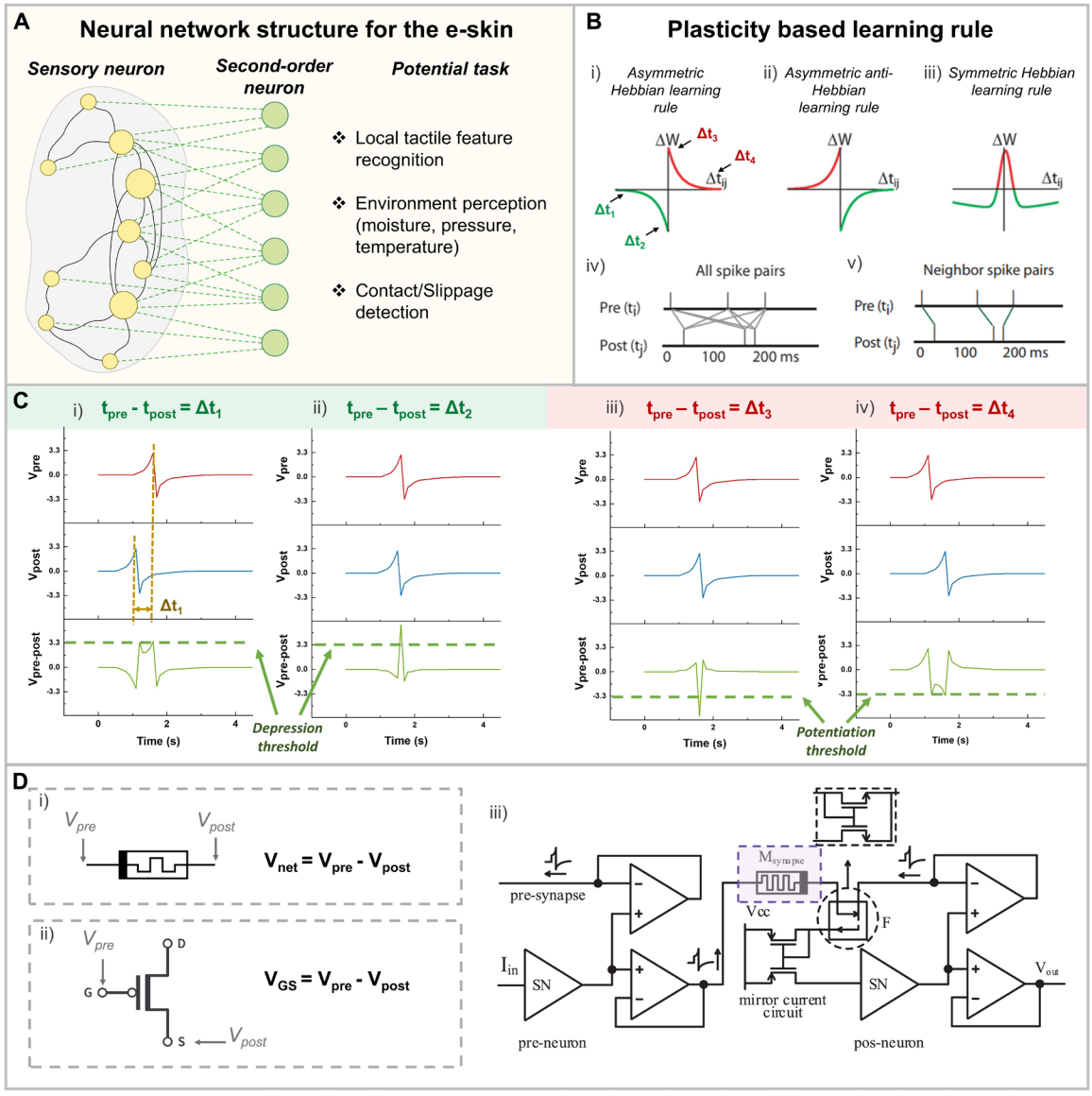


Fig. 5. The neural network structure and learning algorithms for the proposed computational e-skin. (**A**) The neural network structure and the potential tasks it should address. A network similar to reservoir computing has been proposed. However, for e-skin, it should be more complicated because the weights in the first layer along with the receptive fields of the sensory neurons are dependent on the mechanical stimuli. (**B**) Plasticity-based learning rule, STDP, for unsupervised learning. Various forms of STDP have been identified. Typical examples include asymmetry Hebbian learning, asymmetry anti-Hebbian learning, and symmetric Hebbian learning. Reprint from (*135*). (**C**) Waveform engineering is one popular strategy for achieving hardware realization of the STDP learning rule using novel devices such as memristors and synaptic transistors shown in [D (i)] and [D (ii)]. For this, the principle is to take advantage of the net bias across the device, V_{pre}-V_{post}, under various timing. When the net bias is larger than the threshold of the device needed to trigger the synaptic behavior (potentiation or depression), the weight (conductance) of the device would be changed. (**D**) The possible circuit layout for realizing STDP learning for two-terminal memristor and three-terminal synaptic transistor. Adapted from (*136*).

learning (Fig. 5B) (*134*, *135*). The implementation of such a learning rule is hardware-friendly, especially with the previously mentioned synaptic devices. The change of the synaptic weight is only subjected to the time correlation between paired spikes from the pre- and post-neurons, under various pairing schemes such as "nearest neighbor takes all," "nearest neighbor takes more," or "all spike pairs count equally" (Fig. 5B) (*135*). This could be potentially promising for implementation on the soft computational e-skin. For example, for memristor-based synapses, the pre- and post-neuron signals are fed into the two ends of the memristor devices. The net bias across the memristor device is therefore the temporal subtraction of the pre- and post-neuron spikes (Fig. 5D) (*136*). Thus, the difference in the spike timing between the pre- and post-neurons would lead to a net bias of reverse polarity and varying amplitude (Fig. 5C). Depending on the relationship between the potentiation/depression threshold and the net bias across the device, the synaptic weight is modified

IMAGE CREDIT: (D) (136)/ELSEVIER

Downloaded from https://www.science.org at Huazhong University of Science and Technology on September 02, 2026

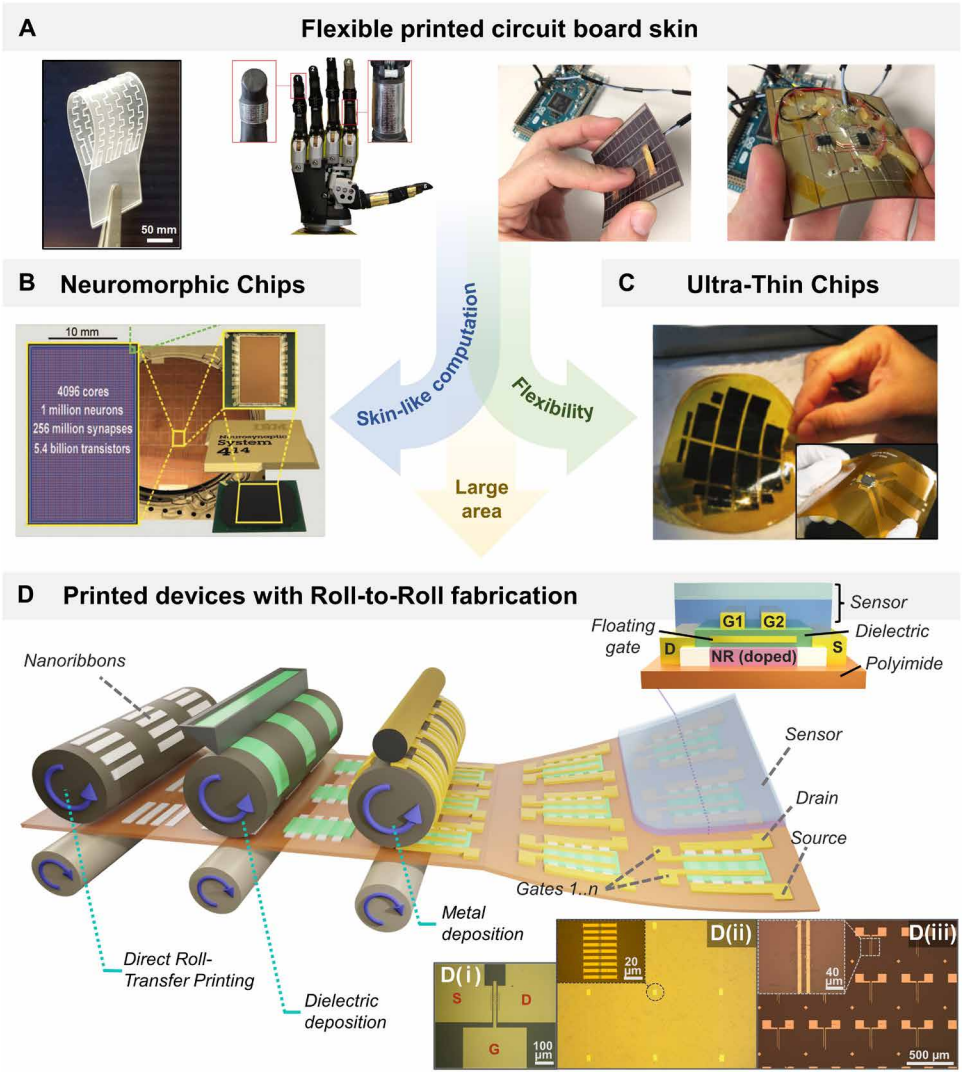


Fig. 6. The technological advances to implement large-area computational e-skin on flexible substrates. (**A**) The energy autonomous e-skin with graphene-based transparent touch-sensing layer on robotic hand and on flexible solar cells. The back side of the solar cells shows rigid off-the-shelf chips. Images adapted from (*192*). (**B**) The neuromorphic chip, TrueNorth, with 1 million spiking neurons implemented using digital electronics. Adapted from (*22*). (**C**) UTC technology could be used to obtain a flexible version of neuromorphic chips and hence the computational e-skin with greater flexibility. Adapted from (*148*, *193*). (**D**) The roll-to-roll printing of various computing building blocks for the future e-skin. The feasibility of such e-skin is evident from the examples of printed electronic layers and devices: (i and ii) transfer printed Si nanoribbons and transistor made from them. Reprint from (*159*). (iii) Contact printed nanowire-based devices. Reprint from (*174*).

accordingly. From the functional viewpoint, the implementation of STDP learning rule could lead to the correlation between two neurons and further possible sensorimotor correlation for robots.

Although unsupervised learning has several benefits, such a learning strategy alone may be insufficient. A method to strengthen the desired behavior and weaken the undesired behavior, based on the environmental feedback, for example, using reinforcement learning, may also be required. In terms of the hardware, reinforcement learning has been demonstrated in the example shown in Fig. 4E and other works using memristor crossbar (or synaptic transistors) and digital circuitry (*137*). However, with respect to the more biologically plausible scenario, SNN, the hardware implementation has not been realized. Possible examples may also exist in the biological nervous system: The synaptic plasticity could be influenced by a global neuromodulator signal. For example, dopamine can lead to facilitation, and acetylcholine can lead to depression. Several computational studies have shown that they could lead to a higher learning accuracy for various tasks (*138*–*141*). In this regard, efforts are needed in the hardware demonstration of the "three-factor STDP behavior" using the artificial synaptic devices, and the devices offering multiple approaches to control the synaptic behavior [chemical and light; (*142*)] could be beneficial.

Power consumption

Because there are a limited number of studies on the power consumption of e-skins, we try to extract data from other scenarios for comparison. For example, the neuromorphic chip "SpiNNaker" contains ~250,000 neurons and 82 million synapses (*143*). It consumes 36 W in total or 20 nJ per synaptic event, at an average firing rate of 22 Hz. The chip "TrueNorth" contains ~1 million neurons and 128 million active synapses, consuming an average of 26 pJ per synaptic event at a firing rate of ~20 Hz (*22*). The e-skin targeting human-level tactile performance would require a similar number of sensory neurons in the first layer as in the case of human skin (~100,000; see Table 1), but with a much less recurrency as compared with SpiNNaker or TrueNorth. Assuming a smaller portion ($\sim^1/_{10}$) of cuneate neurons in the second layer, the power consumption of the proposed e-skin should be in the order of several watts at a moderate firing rate (~20 Hz).

In addition to the power consumption, there are several other problems to consider for developing a computational e-skin. For example, the way to address and send the sensing signal is an aspect for study, because the active or passive matrix manner cannot support the high spatial and temporal resolution at the same time. Another aspect is the method to guarantee the system reliability, because the continuous interaction between the skin and the external environment could possibly lead to localized damage (*144*, *145*).

TOWARD COMPUTATIONAL E-SKIN IMPLEMENTATION

Flexible PCB and chip thinning technology

E-skin needs to be fabricated on soft substrates to mimic the mechanical properties of biological skin. Initial progress has been made

IMAGE CREDIT: (C) (148)/WILEY-VCH

Downloaded from https://www.science.org at Huazhong University of Science and Technology on September 02, 2026

by integrating off-the-shelf sensors and electronic components onto flexible printed circuit boards (PCBs), ranging from hand-based manipulation to the whole-body area, as shown in Fig. 1. Similar approaches could be adopted for computational e-skin by interfacing sensors with neuromorphic chips (Fig. 6, A and B). The neuromorphic chips offer a platform of dense, interconnected neural network that can carry out various computing tasks required by robots (*146*, *147*). Such an arrangement will enable "in-hardware" computing capability in the e-skin using deep neural networks. This is different from the strategy we have discussed so far to develop the "skin-type" tactile functionality, because the achievement of the human-level tactile sensation and perception relies on the intricate interplay between the softness of the skin and the spiking response of the neurons, using a "shallow" network of two layers.

The integration of soft and rigid materials limits the bendability. Furthermore, the mismatch in their mechanical properties increases the chances of failure during extended use. As a result, it is challenging to use hybrid devices on sensitive body parts such as fingertips of a robot, where high-density tactile feedback is required for interaction and manipulation. This can be potentially mitigated through wafer thinning technology using ultrathin chip (UTC) (*148*–*151*), as shown in Fig. 6C. The thin chips bonded onto flexible PCBs could offer greater flexibility. With this strategy, one critical challenge is the lack of suitable bonding techniques to gain access to the circuitry on thin chips from a soft platform. The conventional chip bonding methods are not suitable because they are likely to introduce cracks in the chips. These issues could be resolved by methods such as bonding by printing (*152*–*156*). The challenges related to reliable interconnects could be addressed by mechanically flexible conductive materials such as liquid metals (*157*). Overall, despite these challenges and limitations, using UTCs with flexible PCB is possibly the quickest route toward the realization of the computational e-skin.

Printed electronics on soft substrates

The proposed e-skin can also be fabricated directly on soft platforms, using printing technology with both inorganic (*158*, *159*) and organic (*158*, *160*) materials (Fig. 6D). This will also be an attractive direction for future electronics, because resource-efficient manufacturing could help to reduce electronic waste and contribute to sustainability. Further, it is easier to process biodegradable materials using printing technology so that the printing technology also holds promise for future transient electronics (*161*–*163*). Several printing techniques that are available today include inkjet printing (*118*, *164*–*166*), transfer printing (*159*, *167*–*170*), contact printing (*171*–*174*), and screen printing (*175*–*179*). Specifically, the transfer and contact printing techniques are promising for high-performance electronics and also compatible with roll-to-roll manufacturing (*180*). Figure 6D shows an example of roll-to-roll printed multigate devices (Fig. 3E) on the flexible substrate along with various other building blocks required for the computational e-skin mentioned in the "Computational building blocks and their hardware implementation" section. Specifically, the synaptic device can be made from printed metal-oxide nanowires [Fig. 6D (iii)] (*174*), and the channel of the multigate devices (as nonspiking neuron) can be made of Si nanoribbons (*181*) shown in Fig. 6D (i and ii) (inset). The multigate device has the inputs fed from the readout circuit from various sensors, showing a simple tactile sensing scheme capable of delivering linear summation on the flexible substrate. The low-temperature processing from the printed electronics is naturally compatible with the thermally sensitive soft substrates. However, it should be noted that the printed electronics is still mainly developed within laboratories with limited device metrics such as device density, uniformity, and mobility. Taking the fabrication of FETs as an example, the largest number of printed FETs on the flexible or stretchable substrates is in the order of a few thousand (*182*). Using standard microfabrication techniques, this number can be in the order of tens of thousands (*183*). At present, printing technology could possibly be used to produce those parts of the e-skin that require lower device density, which corresponds to the part of the skin with a lower density of mechanoreceptors or spatial acuity.

CONCLUSION

Next-generation robots are expected to be highly intelligent and autonomous, and the sense of touch is critical for them to safely interact in dynamic, unstructured, and often uncertain environments. For intelligent systems to have human levels of performance, it is vital to develop a sensitive tactile sensory system that provides at least similar information. To attain this, there is a need to expand the e-skin research toward perception and learning. Now, most of the e-skin research still focuses on the tactile sensation and their integration on substrates, which can conform to curvy surfaces of robotic body. We address this need in this review article by focusing on the computational aspect of the skin and the associated PNS to efficiently process the tactile data. The e-skin that can mimic the biological tactile neural pathway could offer the desired preliminary perception capability, markedly decreasing the cognitive load on their central control units. This is analogous to the PNS complementing the functionality of the CNS in humans. We discussed the possible building blocks of the tactile neural pathways and the integration that could imitate their functionality. It is highlighted that the mechanical properties of the skin and the neurological behaviors are correlated in both tactile sensation and perception. Furthermore, we have also discussed how the e-skin development could benefit from advances in areas such as printed and flexible electronics. By revisiting the discoveries from diverse disciplines and reviewing the state-of-the-art in tactile sensing and neuromorphic computing hardware, it is hoped that this article will inspire future advances for the e-skin research, rendering the robots with human-like responsiveness.

REFERENCES AND NOTES

1. M. Kaboli, G. Cheng, Robust tactile descriptors for discriminating objects from textural properties via artificial robotic skin. *IEEE Trans. Robot.* **34**, 985–1003 (2018).
2. R. Dahiya, N. Yogeswaran, F. Liu, L. Manjakkal, E. Burdet, V. Hayward, H. Jorntell, Large-area soft e-skin: The challenges beyond sensor designs. *Proc. IEEE* **107**, 2016–2033 (2019).
3. R. S. Johansson, G. Westling, Roles of glabrous skin receptors and sensorimotor memory in automatic control of precision grip when lifting rougher or more slippery objects. *Exp. Brain Res.* **56**, 550–564 (1984).
4. R. Dahiya, M. Valle, *Robotic Tactile Sensing: Technologies and System* (Springer Science + Business Media, 2013).
5. N. Yogeswaran, W. Dang, W. T. Navaraj, D. Shakthivel, S. Khan, E. O. Polat, S. Gupta, H. Heidari, M. Kaboli, L. Lorenzelli, G. Cheng, R. Dahiya, New materials and advances in making electronic skin for interactive robots. *Adv. Robot.* **29**, 1359–1373 (2015).
6. R. A. Nawrocki, N. Matsuhisa, T. Yokota, T. Someya, 300-nm imperceptible, ultraflexible, and biocompatible e-skin fit with tactile sensors and organic transistors. *Adv. Electron. Mater.* **2**, 1500452 (2016).
7. O. Ozioko, R. Dahiya, Smart tactile gloves for haptic interaction, communication and rehabilitation. *Adv. Intell. Syst.* **4**, 2100091 (2022).
8. O. Ozioko, P. Karipoth, M. Hersh, R. Dahiya, Wearable assistive tactile communication interface based on integrated touch sensors and actuators. *IEEE Trans. Neural Syst. Rehabil. Eng.* **28**, 1344–1352 (2020).

Downloaded from https://www.science.org at Huazhong University of Science and Technology on September 02, 2026

9. M. Kaltenbrunner, T. Sekitani, J. Reeder, T. Yokota, K. Kuribara, T. Tokuhara, M. Drack, R. Schwödiauer, I. Graz, S. Bauer-Gogonea, S. Bauer, T. Someya, An ultra-lightweight design for imperceptible plastic electronics. *Nature* **499**, 458–463 (2013).
10. P. Karipoth, A. Christou, A. Pullanchiyodan, R. Dahiya, Bioinspired inchworm and earthworm like soft robots with intrinsic strain sensing. *Adv. Intell. Syst.* **4**, 2100092 (2022).
11. O. Ozioko, P. Karipoth, P. Escobedo, M. Ntagios, A. Pullanchiyodan, R. Dahiya, SensAct: The soft and squishy tactile sensor with integrated flexible actuator. *Adv. Intell. Syst.* **3**, 1900145 (2021).
12. S. Somlor, R. S. Hartanto, A. Schmitz, S. Sugano, A novel tri-axial capacitive-type skin sensor. *Adv. Robot.* **29**, 1375–1391 (2015).
13. B. Ward-Cherrier, N. Pestell, L. Cramphorn, B. Winstone, M. E. Giannaccini, J. Rossiter, N. F. Lepora, The tactip family: Soft optical tactile sensors with 3d-printed biomimetic morphologies. *Soft Robot.* **5**, 216–227 (2018).
14. R. S. Dahiya, A. Adami, L. Pinna, C. Collini, M. Valle, L. Lorenzelli, Tactile sensing chips with POSFET array and integrated interface electronics. *IEEE Sens. J.* **14**, 3448–3457 (2014).
15. N. Yogeswaran, E. S. Hosseini, R. Dahiya, Graphene based low voltage field effect transistor coupled with biodegradable piezoelectric material based dynamic pressure sensor. *ACS Appl. Mater. Interfaces* **12**, 54035–54040 (2020).
16. D. Hughes, N. Correll, Texture recognition and localization in amorphous robotic skin. *Bioinspir. Biomim.* **10**, 055002 (2015).
17. W. Navaraj, R. Dahiya, Fingerprint-enhanced capacitive-piezoelectric flexible sensing skin to discriminate static and dynamic tactile stimuli. *Adv. Intell. Syst.* **1**, 1900051 (2019).
18. Q. Li, O. Kroemer, Z. Su, F. F. Veiga, M. Kaboli, H. J. Ritter, A review of tactile information: Perception and action through touch. *IEEE Trans. Robot.* **36**, 1619–1634 (2020).
19. G. Thuruthel Thomas, B. Shih, C. Laschi, T. Tolley Michael, Soft robot perception using embedded soft sensors and recurrent neural networks. *Sci. Robot.* **4**, eaav1488 (2019).
20. T. Hellebrekers, N. Chang, K. Chin, M. J. Ford, O. Kroemer, C. Majidi, Soft magnetic tactile skin for continuous force and location estimation using neural networks. *IEEE Robot. Autom. Lett.* **5**, 3892–3898 (2020).
21. M. Kaboli, D. Feng, G. Cheng, Active tactile transfer learning for object discrimination in an unstructured environment using multimodal robotic skin. *Int. J. Humanoid Robot.* **15**, 1850001 (2017).
22. P. A. Merolla, J. V. Arthur, R. Alvarez-Icaza, A. S. Cassidy, J. Sawada, F. Akopyan, B. L. Jackson, N. Imam, C. Guo, Y. Nakamura, B. Brezzo, I. Vo, S. K. Esser, R. Appuswamy, B. Taba, A. Amir, M. D. Flickner, W. P. Risk, R. Manohar, D. S. Modha, A million spiking-neuron integrated circuit with a scalable communication network and interface. *Science* **345**, 668–673 (2014).
23. C. S. Thakur, J. L. Molin, G. Cauwenberghs, G. Indiveri, K. Kumar, N. Qiao, J. Schemmel, R. Wang, E. Chicca, J. Olson Hasler, J. S. Seo, S. Yu, Y. Cao, A. van Schaik, R. Etienne-Cummings, Large-scale neuromorphic spiking array processors: A quest to mimic the brain. *Front. Neurosci.* **12**, 891 (2018).
24. J. Seo, B. Brezzo, Y. Liu, B. C. Parker, S.K. Esser, R. K. Montoye, B. Rajendran, J. Tierno, L. Chang, D. S. Modha, D. J. Friedman, A 45nm CMOS neuromorphic chip with a scalable architecture for learning in networks of spiking neurons, in *2011 IEEE Custom Integrated Circuits Conference (CICC)* (IEEE, 2011), pp. 1–4.
25. M. L. Hammock, A. Chortos, B. C. K. Tee, J. B. H. Tok, Z. Bao, 25th anniversary article: The evolution of electronic skin (E-skin): A brief history, design considerations, and recent progress. *Adv. Mater.* **25**, 5997–6038 (2013).
26. A. Chortos, Z. Bao, Skin-inspired electronic devices. *Mater. Today* **17**, 321–331 (2014).
27. K. Takei, W. Gao, C. Wang, A. Javey, Physical and chemical sensing with electronic skin. *Proc. IEEE* **107**, 2155–2167 (2019).
28. X. Wang, L. Dong, H. Zhang, R. Yu, C. Pan, Z. L. Wang, Recent progress in electronic skin. *Adv. Sci.* **2**, 1500169 (2015).
29. B. Shih, D. Shah, J. Li, T. G. Thuruthel, Y.-L. Park, F. Iida, Z. Bao, R. Kramer-Bottiglio, M. T. Tolley, Electronic skins and machine learning for intelligent soft robots. *Sci. Robot.* **5**, eaaz9239 (2020).
30. J. C. Yang, J. Mun, S. Y. Kwon, S. Park, Z. Bao, S. Park, Electronic skin: Recent progress and future prospects for skin-attachable devices for health monitoring, robotics, and prosthetics. *Adv. Mater.* **31**, 1904765 (2019).
31. S. Luo, J. Bimbo, R. Dahiya, H. Liu, Robotic tactile perception of object properties: A review. *Mechatronics* **48**, 54–67 (2017).
32. R. Mukherjee, P. Ganguly, R. Dahiya, Bioinspired distributed energy in robotics and enabling technologies. *Adv. Intell. Syst.* **2021**, 2100036 (2021).
33. M. Soni, R. Dahiya, Soft eSkin: Distributed touch sensing with harmonized energy and computing. *Philos. Trans. R. Soc. A* **378**, 20190156 (2020).
34. A. Chortos, J. Liu, Z. Bao, Pursuing prosthetic electronic skin. *Nat. Mater.* **15**, 937–950 (2016).
35. M. Wang, Y. Luo, T. Wang, C. Wan, L. Pan, S. Pan, K. He, A. Neo, X. Chen, Artificial skin perception. *Adv. Mater.* **33**, 2003014 (2021).
36. P. Li, H. P. Anwar Ali, W. Cheng, J. Yang, B. C. Tee, Bioinspired prosthetic interfaces. *Adv. Mater. Technol.* **5**, 1900856 (2020).
37. E. R. Kandel, J. H. Schwartz, T. M. Jessell,S. Siegelbaum, A. J. Hudspeth, S. Mack, *Principles of Neural Science* (McGraw-Hill, 2000), vol. 4.
38. V. E. Abraira, D. D. Ginty, The sensory neurons of touch. *Neuron* **79**, 618–639 (2013).
39. M. W. Matlin, H. J. Foley, *Sensation and Perception* (Allyn & Bacon, ed. 3, 1992).
40. D. R. Lesniak, K. L. Marshall, S. A. Wellnitz, B. A. Jenkins, Y. Baba, M. N. Rasband, G. J. Gerling, E. A. Lumpkin, Computation identifies structural features that govern neuronal firing properties in slowly adapting touch receptors. *eLife* **3**, e01488 (2014).
41. C. W. Eurich, H. Schwegler, Coarse coding: Calculation of the resolution achieved by a population of large receptive field neurons. *Biol. Cybern.* **76**, 357–363 (1997).
42. S. Chun, W. Son, H. Kim, S. K. Lim, C. Pang, C. Choi, Self-powered pressure-and vibration-sensitive tactile sensors for learning technique-based neural finger skin. *Nano Lett.* **19**, 3305–3312 (2019).
43. K. Y. Chun, Y. J. Son, E. S. Jeon, S. Lee, C. S. Han, A self-powered sensor mimicking slow- and fast-adapting cutaneous mechanoreceptors. *Adv. Mater.* **30**, 1706299 (2018).
44. V. Hayward, Is there a 'plenhaptic' function? *Philos. Trans. R. Soc. Lond. B Biol. Sci.* **366**, 3115–3122 (2011).
45. J. A. Pruszynski, R. S. Johansson, Edge-orientation processing in first-order tactile neurons. *Nat. Neurosci.* **17**, 1404–1409 (2014).
46. S. C. Liu, T. Delbruck, G. Indiveri, A. Whatley, R. Douglas, *Event-Based Neuromorphic Systems* (John Wiley & Sons, 2014).
47. R. S. Johansson, J. R. Flanagan, Coding and use of tactile signals from the fingertips in object manipulation tasks. *Nat. Rev. Neurosci.* **10**, 345–359 (2009).
48. E. M. Izhikevich, Which model to use for cortical spiking neurons? *IEEE Trans. Neural Netw.* **15**, 1063–1070 (2004).
49. B. C. K. Tee, A. Chortos, A. Berndt, A. K. Nguyen, A. Tom, A. McGuire, Z. C. Lin, K. Tien, W. G. Bae, H. Wang, P. Mei, H. H. Chou, B. Cui, K. Deisseroth, T. N. Ng, Z. Bao, A skin-inspired organic digital mechanoreceptor. *Science* **350**, 313–316 (2015).
50. Y. Kim, A. Chortos, W. Xu, Y. Liu, J. Y. Oh, D. Son, J. Kang, A. M. Foudeh, C. Zhu, Y. Lee, S. Niu, J. Liu, R. Pfattner, Z. Bao, T. W. Lee, A bioinspired flexible organic artificial afferent nerve. *Science* **360**, 998–1003 (2018).
51. Y. Wu, Y. Liu, Y. Zhou, Q. Man, C. Hu, W. Asghar, F. Li, Z. Yu, J. Shang, G. Liu, M. Liao, R.-W. Li, A skin-inspired tactile sensor for smart prosthetics. *Sci. Robot.* **3**, eaat0429 (2018).
52. S. Kim, Y. Lee, H.-D. Kim, S.-J. Choi, A tactile sensor system with sensory neurons and a perceptual synaptic network based on semivolatile carbon nanotube transistors. *NPG Asia Mater.* **12**, 76 (2020).
53. S. Caviglia, L. Pinna, M. Valle, C. Bartolozzi, Spike-based readout of POSFET tactile sensors. *IEEE Trans. Circuits Syst. I Regul. Pap.* **64**, 1421–1431 (2017).
54. T. Birkoben, H. Winterfeld, S. Fichtner, A. Petraru, H. Kohlstedt, A spiking and adapting tactile sensor for neuromorphic applications. *Sci. Rep.* **10**, 17260 (2020).
55. G. Bahuguna, V. S. Adhikary, R. K. Sharma, R. Gupta, Ultrasensitive organic humidity sensor with high specificity for healthcare applications. *Electroanalysis* **32**, 76–85 (2020).
56. M. Teng, Z. Zhou, Y. Qin, Y. Zhao, C. Zhao, J. Cao, A water-soluble fluorescence sensor with high specificity for detecting hydrazine in river water detection and A549 cell imaging. *Sens. Actuators B Chem.* **311**, 127914 (2020).
57. L. Rivas Yepes, E. Demir, J. Y. Lee, R. Sun, M. Smuck, I. E. Araci, Skin mountable capillaric strain sensor with ultrahigh sensitivity and direction specificity. *Adv. Mater. Technol.* **5**, 2000631 (2020).
58. S. Wang, M. Z. Hossain, K. Shinozuka, N. Shimizu, S. Kitada, T. Suzuki, R. Ichige, A. Kuwana, H. Kobayashi, Graphene field-effect transistor biosensor for detection of biotin with ultrahigh sensitivity and specificity. *Biosens. Bioelectron.* **165**, 112363 (2020).
59. L. Zhang, G. Wang, D. Wu, C. Xiong, L. Zheng, Y. Ding, H. Lu, G. Zhang, L. Qiu, Highly selective and sensitive sensor based on an organic electrochemical transistor for the detection of ascorbic acid. *Biosens. Bioelectron.* **100**, 235–241 (2018).
60. W. Gerstner, W. M. Kistler, *Spiking Neuron Models: Single Neurons, Populations, Plasticity* (Cambridge Univ. Press, 2012).
61. A. L. Hodgkin, A. F. Huxley, A quantitative description of membrane current and its application to conduction and excitation in nerve. *J. Physiol.* **117**, 500–544 (1952).
62. E. M. Izhikevich, Simple model of spiking neurons. *IEEE Trans. Neural Netw.* **14**, 1569–1572 (2003).
63. N. Brunel, M. C. Van Rossum, Quantitative investigations of electrical nerve excitation treated as polarization. *Biol. Cybern.* **97**, 341–349 (2007).
64. W. Yi, K. K. Tsang, S. K. Lam, X. Bai, J. A. Crowell, E. A. Flores, Biological plausibility and stochasticity in scalable VO2 active memristor neurons. *Nat. Commun.* **9**, 4661 (2018).
65. H. Liu, T. Wu, X. Yan, J. Wu, N. Wang, Z. du, H. Yang, B. Chen, Z. Zhang, F. Liu, W. Wu, J. Guo, H. Wang, A tantalum disulfide charge-density-wave stochastic artificial neuron for emulating neural statistical properties. *Nano Lett.* **21**, 3465–3472 (2021).
66. P. Stoliar, J. Tranchant, B. Corraze, E. Janod, M. P. Besland, F. Tesler, M. Rozenberg, L. Cario, A leaky-integrate-and-fire neuron analog realized with a Mott Insulator. *Adv. Funct. Mater.* **27**, 1604740 (2017).

Downloaded from https://www.science.org at Huazhong University of Science and Technology on September 02, 2026

67. S. M. Bohaichuk, S. Kumar, G. Pitner, C. J. McClellan, J. Jeong, M. G. Samant, H. S. P. Wong, S. S. P. Parkin, R. S. Williams, E. Pop, Fast spiking of a mott VO_2–Carbon nanotube composite device. *Nano Lett.* **19**, 6751–6755 (2019).
68. Z. Wang, S. Joshi, S. Savel'ev, W. Song, R. Midya, Y. Li, M. Rao, P. Yan, S. Asapu, Y. Zhuo, H. Jiang, P. Lin, C. Li, J. H. Yoon, N. K. Upadhyay, J. Zhang, M. Hu, J. P. Strachan, M. Barnell, Q. Wu, H. Wu, R. S. Williams, Q. Xia, J. J. Yang, Fully memristive neural networks for pattern classification with unsupervised learning. *Nat. Electron.* **1**, 137–145 (2018).
69. Z. Wang, M. Rao, J. W. Han, J. Zhang, P. Lin, Y. Li, C. Li, W. Song, S. Asapu, R. Midya, Y. Zhuo, H. Jiang, J. H. Yoon, N. K. Upadhyay, S. Joshi, M. Hu, J. P. Strachan, M. Barnell, Q. Wu, H. Wu, Q. Qiu, R. S. Williams, Q. Xia, J. J. Yang, Capacitive neural network with neuro-transistors. *Nat. Commun.* **9**, 3208 (2018).
70. C. Mead, *Analog VLSI and Neural Systems* (Addison-Wesley, 1989).
71. I. Sourikopoulos, S. Hedayat, C. Loyez, F. Danneville, V. Hoel, E. Mercier, A. Cappy, A 4-fJ/spike artificial neuron in 65 nm CMOS technology. *Front. Neurosci.* **11**, 123 (2017).
72. J. H. B. Wijekoon, P. Dudek, A CMOS circuit implementation of a spiking neuron with bursting and adaptation on a biological timescale, in *2009 IEEE Biomedical Circuits and Systems Conference* (IEEE, 2009), pp. 193–196.
73. A. van Schaik, Building blocks for electronic spiking neural networks. *Neural Netw.* **14**, 617–628 (2001).
74. G. Indiveri, Synaptic plasticity and spike-based computation in VLSI networks of integrate-and-fire neurons. *Neural Inf. Process. Lett. Rev.* **11**, 135–146 (2007).
75. J. H. B. Wijekoon, P. Dudek, Compact silicon neuron circuit with spiking and bursting behaviour. *Neural Netw.* **21**, 524–534 (2008).
76. M. D. Pickett, R. Stanley Williams, Sub-100 fJ and sub-nanosecond thermally driven threshold switching in niobium oxide crosspoint nanodevices. *Nanotechnology* **23**, 215202 (2012).
77. S. Oh, Y. Shi, J. del Valle, P. Salev, Y. Lu, Z. Huang, Y. Kalcheim, I. K. Schuller, D. Kuzum, Energy-efficient Mott activation neuron for full-hardware implementation of neural networks. *Nat. Nanotechnol.* **16**, 680–687 (2021).
78. W. Taube Navaraj, C. García Núñez, D. Shakthivel, V. Vinciguerra, F. Labeau, D. H. Gregory, R. Dahiya, Nanowire FET based neural element for robotic tactile sensing skin. *Front. Neurosci.* **11**, 501 (2017).
79. H. Jeong, L. Shi, Memristor devices for neural networks. *J. Phys. D* **52**, 023003 (2019).
80. S. Choi, J. Yang, G. Wang, Emerging memristive artificial synapses and neurons for energy-efficient neuromorphic computing. *Adv. Mater.* **32**, 2004659 (2020).
81. X. Pan, T. Jin, J. Gao, C. Han, Y. Shi, W. Chen, Stimuli-enabled artificial synapses for neuromorphic perception: Progress and perspectives. *Small* **16**, 2001504 (2020).
82. F. Chen, Y. Zhou, Y. Zhu, R. Zhu, P. Guan, J. Fan, L. Zhou, N. Valanoor, F. von Wegner, E. Saribatir, I. Birznieks, T. Wan, D. Chu, Recent progress in artificial synaptic devices: Materials, processing and applications. *J. Mater. Chem.* **9**, 8372–8394 (2021).
83. Q. Xia, J. J. Yang, Memristive crossbar arrays for brain-inspired computing. *Nat. Mater.* **18**, 309–323 (2019).
84. S. G. Kim, J. S. Han, H. Kim, S. Y. Kim, H. W. Jang, Recent advances in memristive materials for artificial synapses. *Adv. Mater. Technol.* **3**, 1800457 (2018).
85. F. Zahoor, T. Z. Azni Zulkifli, F. A. Khanday, Resistive random access memory (RRAM): An overview of materials, switching mechanism, performance, multilevel cell (mlc) storage, modeling, and applications. *Nanoscale Res. Lett.* **15**, 90 (2020).
86. W. Zhang, R. Mazzarello, M. Wuttig, E. Ma, Designing crystallization in phase-change materials for universal memory and neuro-inspired computing. *Nat. Rev. Mater.* **4**, 150–168 (2019).
87. A. Athmanathan, M. Stanisavljevic, N. Papandreou, H. Pozidis, E. Eleftheriou, Multilevel-cell phase-change memory: A viable technology. *IEEE J. Emerg. Sel. Top. Circuits Syst.* **6**, 87–100 (2016).
88. S. W. Fong, C. M. Neumann, H. P. Wong, Phase-change memory—Towards a storage-class memory. *IEEE Trans. Electron Devices* **64**, 4374–4385 (2017).
89. D. Apalkov, B. Dieny, J. Slaughter, Magnetoresistive random access memory. *Proc. IEEE* **104**, 1796–1830 (2016).
90. K. Lee, S. Jang, K. L. Kim, M. Koo, C. Park, S. Lee, J. Lee, G. Wang, C. Park, Artificially intelligent tactile ferroelectric skin. *Adv. Sci.* **7**, 2001662 (2020).
91. Y. Li, K.-W. Ang, Hardware implementation of neuromorphic computing using large-scale memristor crossbar arrays. *Adv. Intell. Syst.* **3**, 2000137 (2021).
92. S. Saïghi, C. G. Mayr, T. Serrano-Gotarredona, H. Schmidt, G. Lecerf, J. Tomas, J. Grollier, S. Boyn, A. F. Vincent, D. Querlioz, S. L. Barbera, F. Alibart, D. Vuillaume, O. Bichler, C. Gamrat, B. Linares-Barranco, Plasticity in memristive devices for spiking neural networks. *Front. Neurosci.* **9**, 51 (2015).
93. N. Du, X. Zhao, Z. Chen, B. Choubey, M. D. Ventra, I. Skorupa, D. Bürger, H. Schmidt, Synaptic plasticity in memristive artificial synapses and their robustness against noisy inputs. *Front. Neurosci.* **15**, 696 (2021).
94. S. Kim, C. du, P. Sheridan, W. Ma, S. H. Choi, W. D. Lu, Experimental demonstration of a second-order memristor and its ability to biorealistically implement synaptic plasticity. *Nano Lett.* **15**, 2203–2211 (2015).
95. M. Prezioso, M. R. Mahmoodi, F. M. Bayat, H. Nili, H. Kim, A. Vincent, D. B. Strukov, Spike-timing-dependent plasticity learning of coincidence detection with passively integrated memristive circuits. *Nat. Commun.* **9**, 5311 (2018).
96. Q. Duan, Z. Jing, X. Zou, Y. Wang, K. Yang, T. Zhang, S. Wu, R. Huang, Y. Yang, Spiking neurons with spatiotemporal dynamics and gain modulation for monolithically integrated memristive neural networks. *Nat. Commun.* **11**, 3399 (2020).
97. C. Li, D. Belkin, Y. Li, P. Yan, M. Hu, N. Ge, H. Jiang, E. Montgomery, P. Lin, Z. Wang, W. Song, J. P. Strachan, M. Barnell, Q. Wu, R. S. Williams, J. J. Yang, Q. Xia, Efficient and self-adaptive in-situ learning in multilayer memristor neural networks. *Nat. Commun.* **9**, 2385 (2018).
98. S. K. Kim, Y. J. Jeong, P. Bidenko, H. R. Lim, Y. R. Jeon, H. Kim, Y. J. Lee, D. M. Geum, J. H. Han, C. Choi, H. J. Kim, S. H. Kim, 3D stackable synaptic transistor for 3D integrated artificial neural networks. *ACS Appl. Mater. Interfaces* **12**, 7372–7380 (2020).
99. F. Cai, J. M. Correll, S. H. Lee, Y. Lim, V. Bothra, Z. Zhang, M. P. Flynn, W. D. Lu, A fully integrated reprogrammable memristor–CMOS system for efficient multiply–accumulate operations. *Nat. Electron.* **2**, 290–299 (2019).
100. P. Yao, H. Wu, B. Gao, J. Tang, Q. Zhang, W. Zhang, J. J. Yang, H. Qian, Fully hardware-implemented memristor convolutional neural network. *Nature* **577**, 641–646 (2020).
101. S. Ambrogio, S. Balatti, V. Milo, R. Carboni, Z. Q. Wang, A. Calderoni, N. Ramaswamy, D. Ielmini, Neuromorphic learning and recognition with one-transistor-one-resistor synapses and bistable metal oxide RRAM. *IEEE Trans. Electron Devices* **63**, 1508–1515 (2016).
102. D. Zhang, C. H. Yeh, W. Cao, K. Banerjee, 0.5T0.5R—An ultracompact RRAM cell uniquely enabled by van der waals heterostructures. *IEEE Trans. Electron Devices* **68**, 2033–2040 (2021).
103. H. Abbas, Y. Abbas, G. Hassan, A. S. Sokolov, Y. R. Jeon, B. Ku, C. J. Kang, C. Choi, The coexistence of threshold and memory switching characteristics of ALD HfO_2 memristor synaptic arrays for energy-efficient neuromorphic computing. *Nanoscale* **12**, 14120–14134 (2020).
104. S. Yu, Neuro-inspired computing with emerging nonvolatile memorys. *Proc. IEEE* **106**, 260–285 (2018).
105. S. Dai, Y. Zhao, Y. Wang, J. Zhang, L. Fang, S. Jin, Y. Shao, J. Huang, Recent advances in transistor-based artificial synapses. *Adv. Funct. Mater.* **29**, 1903700 (2019).
106. S. Wang, C. Chen, Z. Yu, Y. He, X. Chen, Q. Wan, Y. Shi, D. W. Zhang, H. Zhou, X. Wang, P. Zhou, A MoS2/PTCDA hybrid heterojunction synapse with efficient photoelectric dual modulation and versatility. *Adv. Mater.* **31**, 1806227 (2019).
107. H. Ling, D. A. Koutsouras, S. Kazemzadeh, Y. van de Burgt, F. Yan, P. Gkoupidenis, Electrolyte-gated transistors for synaptic electronics, neuromorphic computing, and adaptable biointerfacing. *Appl. Phys. Rev.* **7**, 011307 (2020).
108. L. Van Tho, K.-J. Baeg, Y.-Y. Noh, Organic nano-floating-gate transistor memory with metal nanoparticles. *Nano Converg.* **3**, 10 (2016).
109. J. Y. Gerasimov, R. Gabrielsson, R. Forchheimer, E. Stavrinidou, D. T. Simon, M. Berggren, S. Fabiano, An evolvable organic electrochemical transistor for neuromorphic applications. *Adv. Sci.* **6**, 1801339 (2019).
110. S. Bhattacharjee, R. Wigchering, H. G. Manning, J. J. Boland, P. K. Hurley, Emulating synaptic response in n- and p-channel MoS2 transistors by utilizing charge trapping dynamics. *Sci. Rep.* **10**, 12178 (2020).
111. S. Dai, X. Wu, D. Liu, Y. Chu, K. Wang, B. Yang, J. Huang, Light-stimulated synaptic devices utilizing interfacial effect of organic field-effect transistors. *ACS Appl. Mater. Interfaces* **10**, 21472–21480 (2018).
112. H. K. Li, T. P. Chen, P. Liu, S. G. Hu, Y. Liu, Q. Zhang, P. S. Lee, A light-stimulated synaptic transistor with synaptic plasticity and memory functions based on $InGaZnO_x$–Al_2O_3 thin film structure. *J. Appl. Phys.* **119**, 244505 (2016).
113. J. Yu, G. Gao, J. Huang, X. Yang, J. Han, H. Zhang, Y. Chen, C. Zhao, Q. Sun, Z. L. Wang, Contact-electrification-activated artificial afferents at femtojoule energy. *Nat. Commun.* **12**, 1581 (2021).
114. Y. Zang, H. Shen, D. Huang, C.-A. Di, D. Zhu, A dual-organic-transistor-based tactile-perception system with signal-processing functionality. *Adv. Mater.* **29**, 1606088 (2017).
115. K. Berggren, Q. Xia, K. K. Likharev, D. B. Strukov, H. Jiang, T. Mikolajick, D. Querlioz, M. Salinga, J. R. Erickson, S. Pi, F. Xiong, P. Lin, C. Li, Y. Chen, S. Xiong, B. D. Hoskins, M. W. Daniels, A. Madhavan, J. A. Liddle, J. J. McClelland, Y. Yang, J. Rupp, S. S. Nonnenmann, K.-T. Cheng, N. Gong, M. A. Lastras-Montaño, A. A. Talin, A. Salleo, B. J. Shastri, T. F. de Lima, P. Prucnal, A. N. Tait, Y. Shen, H. Meng, C. Roques-Carmes, Z. Cheng, H. Bhaskaran, D. Jariwala, H. Wang, J. M. Shainline, K. Segall, J. J. Yang, K. Roy, S. Datta, A. Raychowdhury, Roadmap on emerging hardware and technology for machine learning. *Nanotechnology* **32**, 012002 (2021).
116. H. Wan, Y. Cao, L. W. Lo, J. Zhao, N. Sepúlveda, C. Wang, Flexible carbon nanotube synaptic transistor for neurological electronic skin applications. *ACS Nano* **14**, 10402–10412 (2020).

Downloaded from https://www.science.org at Huazhong University of Science and Technology on September 02, 2026

117. H. Shim, K. Sim, F. Ershad, P. Yang, A. Thukral, Z. Rao, H.-J. Kim, Y. Liu, X. Wang, G. Gu, L. Gao, X. Wang, Y. Chai, C. Yu, Stretchable elastic synaptic transistors for neurologically integrated soft engineering systems. *Sci. Adv.* **5**, eaax4961 (2019).
118. F. Molina-Lopez, T. Z. Gao, U. Kraft, C. Zhu, T. Öhlund, R. Pfattner, V. R. Feig, Y. Kim, S. Wang, Y. Yun, Z. Bao, Inkjet-printed stretchable and low voltage synaptic transistor array. *Nat. Commun.* **10**, 2676 (2019).
119. X. Feng, Y. Li, L. Wang, S. Chen, Z. G. Yu, W. C. Tan, N. Macadam, G. Hu, L. Huang, L. Chen, X. Gong, D. Chi, T. Hasan, A. V. Y. Thean, Y. W. Zhang, K. W. Ang, A fully printed flexible MoS_2 memristive artificial synapse with femtojoule switching energy. *Adv. Electron. Mater.* **5**, 1900740 (2019).
120. X. Yan, Z. Zhou, J. Zhao, Q. Liu, H. Wang, G. Yuan, J. Chen, Flexible memristors as electronic synapses for neuro-inspired computation based on scotch tape-exfoliated mica substrates. *Nano Res.* **11**, 1183–1192 (2018).
121. C. Wu, T. W. Kim, H. Y. Choi, D. B. Strukov, J. J. Yang, Flexible three-dimensional artificial synapse networks with correlated learning and trainable memory capability. *Nat. Commun.* **8**, 752 (2017).
122. W. Huh, D. Lee, C.-H. Lee, Memristors based on 2D materials as an artificial synapse for neuromorphic electronics. *Adv. Mater.* **32**, 2002092 (2020).
123. Y. Lee, J. Y. Oh, W. Xu, O. Kim, T. R. Kim, J. Kang, Y. Kim, D. Son, J. B.-H. Tok, M. J. Park, Z. Bao, T.-W. Lee, Stretchable organic optoelectronic sensorimotor synapse. *Sci. Adv.* **4**, eaat7387 (2018).
124. T. Okatani, H. Takahashi, T. Takahata, I. Shimoyama, Evaluation of ground slippery condition during walk of bipedal robot using MEMS slip sensor, in *2017 IEEE 30th International Conference on Micro Electro Mechanical Systems (MEMS)* (IEEE, 2017), pp. 1033–1035.
125. A. G. Eguíluz, I. Rañó, S. A. Coleman, T. M. McGinnity, Reliable robotic handovers through tactile sensing. *Auton. Robot.* **43**, 1623–1637 (2019).
126. S. J. Huston, V. Jayaraman, Studying sensorimotor integration in insects. *Curr. Opin. Neurobiol.* **21**, 527–534 (2011).
127. I. Krauhausen, D. A. Koutsouras, A. Melianas, S. T. Keene, K. Lieberth, H. Ledanseur, R. Sheelamanthula, A. Giovannitti, F. Torricelli, I. Mcculloch, P. W. M. Blom, A. Salleo, Y. van de Burgt, P. Gkoupidenis, Organic neuromorphic electronics for sensorimotor integration and learning in robotics. *Sci. Adv.* **7**, eabl5068 (2021).
128. F. Liu, S. Deswal, A. Christou, M. S. Baghini, R. Chirila, D. Shakthivel, M. Chakraborty, R. Dahiya, Printed synaptic transistors based electronic skin for robots to feel and learn. *Sci. Robot.* **7**, eabl7286 (2022).
129. A. Zylberberg, D. Fernández Slezak, P. R. Roelfsema, S. Dehaene, M. Sigman, The brain's router: A cortical network model of serial processing in the primate brain. *PLOS Comput. Biol.* **6**, e1000765 (2010).
130. H. P. Saal, B. P. Delhaye, B. C. Rayhaun, S. J. Bensmaia, Simulating tactile signals from the whole hand with millisecond precision. *Proc. Natl. Acad. Sci. U.S.A.* **114**, E5693–E5702 (2017).
131. F. Vega-Bermudez, K. Johnson, SA1 and RA receptive fields, response variability, and population responses mapped with a probe array. *J. Neurophysiol.* **81**, 2701–2710 (1999).
132. Z. Wang, C. Li, P. Lin, M. Rao, Y. Nie, W. Song, Q. Qiu, Y. Li, P. Yan, J. P. Strachan, N. Ge, N. McDonald, Q. Wu, M. Hu, H. Wu, R. S. Williams, Q. Xia, J. J. Yang, In situ training of feed-forward and recurrent convolutional memristor networks. *Nat. Mach. Intell.* **1**, 434–442 (2019).
133. M. Prezioso, F. Merrikh-Bayat, B. D. Hoskins, G. C. Adam, K. K. Likharev, D. B. Strukov, Training and operation of an integrated neuromorphic network based on metal-oxide memristors. *Nature* **521**, 61–64 (2015).
134. K. Buchanan, J. Mellor, The activity requirements for spike timing-dependent plasticity in the hippocampus. *Front. Synaptic Neurosci.* **2**, 11 (2010).
135. H. Shouval, S. Wang, G. Wittenberg, Spike timing dependent plasticity: A consequence of more fundamental learning rules. *Front. Comput. Neurosci.* **4**, 19 (2010).
136. L. Zhao, Q. Hong, X. Wang, Novel designs of spiking neuron circuit and STDP learning circuit based on memristor. *Neurocomputing* **314**, 207–214 (2018).
137. Z. Wang, C. Li, W. Song, M. Rao, D. Belkin, Y. Li, P. Yan, H. Jiang, P. Lin, M. Hu, J. P. Strachan, N. Ge, M. Barnell, Q. Wu, A. G. Barto, Q. Qiu, R. S. Williams, Q. Xia, J. J. Yang, Reinforcement learning with analogue memristor arrays. *Nat. Electron.* **2**, 115–124 (2019).
138. J. N. J. Reynolds, B. I. Hyland, J. R. Wickens, A cellular mechanism of reward-related learning. *Nature* **413**, 67–70 (2001).
139. V. Pawlak, J. N. D. Kerr, Dopamine receptor activation is required for corticostriatal spike-timing-dependent plasticity. *J. Neurosci.* **28**, 2435–2446 (2008).
140. M. Mikaitis, G. Pineda García, J. C. Knight, S. B. Furber, Neuromodulated synaptic plasticity on the SpiNNaker neuromorphic system. *Front. Neurosci.* **12**, 105 (2018).
141. R. S. Sutton, A. G. Barto, *Introduction to Reinforcement Learning* (MIT Press, ed. 1, 1998).
142. C. Shen, X. Gao, C. Chen, S. Ren, J.-L. Xu, Y.-D. Xia, S.-D. Wang, ZnO nanowire optoelectronic synapse for neuromorphic computing. *Nanotechnology* **33**, 065205 (2022).
143. E. Painkras, L. A. Plana, J. Garside, S. Temple, F. Galluppi, C. Patterson, D. R. Lester, A. D. Brown, S. B. Furber, SpiNNaker: A 1-W 18-core system-on-chip for massively-parallel neural network simulation. *IEEE J. Solid-State Circuits* **48**, 1943–1953 (2013).
144. W. W. Lee, Y. J. Tan, H. Yao, S. Li, H. H. See, M. Hon, K. A. Ng, B. Xiong, J. S. Ho, B. C. K. Tee, A neuro-inspired artificial peripheral nervous system for scalable electronic skins. *Sci. Robot.* **4**, eaax2198 (2019).
145. C. Bader, F. Bergner, G. Cheng, A robust and efficient dynamic network protocol for a large-scale artificial robotic skin, in *2018 IEEE/RSJ International Conference on Intelligent Robots and Systems (IROS)* (IEEE, 2018), pp. 1600–1605.
146. Y. Ohmura, Y. Kuniyoshi, Humanoid robot which can lift a 30kg box by whole body contact and tactile feedback, in *2007 IEEE/RSJ International Conference on Intelligent Robots and Systems* (IEEE, 2007), pp. 1136–1141.
147. G. Cheng, E. Dean-Leon, F. Bergner, J. Rogelio Guadarrama Olvera, Q. Leboutet, P. Mittendorfer, A comprehensive realization of robot skin: Sensors, sensing, control, and applications. *Proc. IEEE* **107**, 2034–2051 (2019).
148. W. T. Navaraj, S. Gupta, L. Lorenzelli, R. Dahiya, Wafer scale transfer of ultrathin silicon chips on flexible substrates for high performance bendable systems. *Adv. Electron. Mater.* **4**, 1700277 (2018).
149. S. Gupta, W. T. Navaraj, L. Lorenzelli, R. Dahiya, Ultra-thin chips for high-performance flexible electronics. *npj Flex. Electron.* **2**, 8 (2018).
150. A. Vilouras, A. Christou, L. Manjakkal, R. Dahiya, Ultrathin ion-sensitive field-effect transistor chips with bending-induced performance enhancement. *ACS Appl. Electron. Mater.* **2**, 2601–2610 (2020).
151. A. S. Dahiya, D. Shakthivel, Y. Kumaresan, A. Zumeit, A. Christou, R. Dahiya, High-performance printed electronics based on inorganic semiconducting nano to chip scale structures. *Nano Converg.* **7**, 33 (2020).
152. T. Seifert, M. Baum, F. Roscher, M. Wiemer, T. Gessner, Aerosol jet printing of nano particle based electrical chip interconnects. *Mater. Today Proc.* **2**, 4262–4271 (2015).
153. J. Wang, R. C. Y. Auyeung, H. Kim, N. A. Charipar, A. Piqué, Three-dimensional printing of interconnects by laser direct-write of silver nanopastes. *Adv. Mater.* **22**, 4462–4466 (2010).
154. H.-L. Kang, S. M. Sim, Y. Lee, J. H. Yu, K. Y. Shin, S. H. Lee, J. M. Kim, Flip chip bonding using ink-jet printing technology. *Microsyst. Technol.* **25**, 4753–4759 (2019).
155. H. Y. Zhang, X. Li, H. N. Jiang, Y. H. Mei, G. Q. Lu, Large-area substrate bonding with single-printing silver paste sintering for power modules. *IEEE Trans. Compon. Packag. Manuf. Technol.* **11**, 11–18 (2021).
156. S. Ma, Y. Kumaresan, A. S. Dahiya, R. Dahiya, Ultra-thin chips with printed interconnects on flexible foils. *Adv. Electron. Mater.* **8**, 2101029 (2021).
157. Y.-G. Park, H. Min, H. Kim, A. Zhexembekova, C. Y. Lee, J. U. Park, Three-dimensional, high-resolution printing of carbon nanotube/liquid metal composites with mechanical and electrical reinforcement. *Nano Lett.* **19**, 4866–4872 (2019).
158. A. Carlson, A. M. Bowen, Y. Huang, R. G. Nuzzo, J. A. Rogers, Transfer printing techniques for materials assembly and micro/nanodevice fabrication. *Adv. Mater.* **24**, 5284–5318 (2012).
159. A. Zumeit, A. Dahiya, A. Christou, D. Shakthivel, R. Dahiya, Direct roll transfer printed silicon nanoribbon arrays based high-performance flexible electronics. *npj Flex. Electron.* **5**, 18 (2021).
160. T. Sekitani, U. Zschieschang, H. Klauk, T. Someya, Flexible organic transistors and circuits with extreme bending stability. *Nat. Mater.* **9**, 1015–1022 (2010).
161. E. S. Hosseini, S. Dervin, P. Ganguly, R. Dahiya, Biodegradable materials for sustainable health monitoring devices. *ACS Appl. Bio Mater.* **4**, 163–194 (2021).
162. J. K. Chang, H. P. Chang, Q. Guo, J. Koo, C. I. Wu, J. A. Rogers, Biodegradable electronic systems in 3D, heterogeneously integrated formats. *Adv. Mater.* **30**, 1704955 (2018).
163. M. Chakraborty, J. Kettle, R. Dahiya, Electronic waste reduction through devices and printed circuit boards designed for circularity. *IEEE J. Flex. Electron.* **1**, 4–23 (2022).
164. J. A. Rogers, Z. Bao, Printed plastic electronics and paperlike displays. *J. Polym. Sci. A Polym. Chem.* **40**, 3327–3334 (2002).
165. U. Kraft, F. Molina-Lopez, D. Son, Z. Bao, B. Murmann, Ink development and printing of conducting polymers for intrinsically stretchable interconnects and circuits. *Adv. Electron. Mater.* **6**, 1900681 (2020).
166. C. Kotlowski, P. Aspermair, H. U. Khan, C. Reiner-Rozman, J. Breu, S. Szunerits, J. J. Kim, Z. Bao, C. Kleber, P. Pelosi, W. Knoll, Electronic biosensing with flexible organic transistor devices. *Flex. Print. Electron.* **3**, 034003 (2018).
167. T.-H. Kim, A. Carlson, J. H. Ahn, S. M. Won, S. Wang, Y. Huang, J. A. Rogers, Kinetically controlled, adhesiveless transfer printing using microstructured stamps. *Appl. Phys. Lett.* **94**, 113502 (2009).
168. C. Linghu, S. Zhang, C. Wang, J. Song, Transfer printing techniques for flexible and stretchable inorganic electronics. *npj Flex. Electron* **2**, 26 (2018).
169. M. A. Meitl, Z. T. Zhu, V. Kumar, K. J. Lee, X. Feng, Y. Y. Huang, I. Adesida, R. G. Nuzzo, J. A. Rogers, Transfer printing by kinetic control of adhesion to an elastomeric stamp. *Nat. Mater.* **5**, 33–38 (2006).

Downloaded from https://www.science.org at Huazhong University of Science and Technology on September 02, 2026

170. R. S. Cok, J. W. Hamer, C. A. Bower, E. Menard, S. Bonafede, AMOLED displays with transfer-printed integrated circuits. *J. Soc. Inf. Disp.* **19**, 335–341 (2011).
171. Z. Fan, J. C. Ho, Z. A. Jacobson, R. Yerushalmi, R. L. Alley, H. Razavi, A. Javey, Wafer-scale assembly of highly ordered semiconductor nanowire arrays by contact printing. *Nano Lett.* **8**, 20–25 (2008).
172. T. Takahashi, K. Takei, J. C. Ho, Y. L. Chueh, Z. Fan, A. Javey, Monolayer resist for patterned contact printing of aligned nanowire arrays. *J. Am. Chem. Soc.* **131**, 2102–2103 (2009).
173. D. Roßkopf, S. Strehle, Surface-controlled contact printing for nanowire device fabrication on a large scale. *Nanotechnology* **27**, 185301 (2016).
174. A. Christou, F. Liu, R. Dahiya, Development of a highly controlled system for large-area, directional printing of quasi-1D nanomaterials. *Microsyst. Nanoeng.* **7**, 82 (2021).
175. J. Suikkola, T. Björninen, M. Mosallaei, T. Kankkunen, P. Iso-Ketola, L. Ukkonen, J. Vanhala, M. Mäntysalo, Screen-printing fabrication and characterization of stretchable electronics. *Sci. Rep.* **6**, 25784 (2016).
176. W. J. Hyun, E. B. Secor, M. C. Hersam, C. D. Frisbie, L. F. Francis, High-resolution patterning of graphene by screen printing with a silicon stencil for highly flexible printed electronics. *Adv. Mater.* **27**, 109–115 (2015).
177. P. He, J. Cao, H. Ding, C. Liu, J. Neilson, Z. Li, I. A. Kinloch, B. Derby, Screen-printing of a highly conductive graphene ink for flexible printed electronics. *ACS Appl. Mater. Interfaces* **11**, 32225–32234 (2019).
178. X. Cao, H. Chen, X. Gu, B. Liu, W. Wang, Y. Cao, F. Wu, C. Zhou, Screen printing as a scalable and low-cost approach for rigid and flexible thin-film transistors using separated carbon nanotubes. *ACS Nano* **8**, 12769–12776 (2014).
179. R. Parashkov, E. Becker, T. Riedl, H. Johannes, W. Kowalsky, Large area electronics using printing methods. *Proc. IEEE* **93**, 1321–1329 (2005).
180. R. Yerushalmi, Z. A. Jacobson, J. C. Ho, Z. Fan, A. Javey, Large scale, highly ordered assembly of nanowire parallel arrays by differential roll printing. *Appl. Phys. Lett.* **91**, 203104 (2007).
181. A. Zumeit, W. T. Navaraj, D. Shakthivel, R. Dahiya, Nanoribbon-based flexible high-performance transistors fabricated at room temperature. *Adv. Electron. Mater.* **6**, 1901023 (2020).
182. S. Wang, J. Xu, W. Wang, G. J. N. Wang, R. Rastak, F. Molina-Lopez, J. W. Chung, S. Niu, V. R. Feig, J. Lopez, T. Lei, S. K. Kwon, Y. Kim, A. M. Foudeh, A. Ehrlich, A. Gasperini, Y. Yun, B. Murmann, J. B. H. Tok, Z. Bao, Skin electronics from scalable fabrication of an intrinsically stretchable transistor array. *Nature* **555**, 83–88 (2018).
183. J. Biggs, J. Myers, J. Kufel, E. Ozer, S. Craske, A. Sou, C. Ramsdale, K. Williamson, R. Price, S. White, A natively flexible 32-bit Arm microprocessor. *Nature* **595**, 532–536 (2021).
184. M. Raibert, An all digital VLSI tactile array sensor, in *Proceedings of the 1984 IEEE International Conference on Robotics and Automation* (IEEE, 1984), vol. 1, pp. 314–319.
185. V. J. Lumelsky, M. S. Shur, S. Wagner, Sensitive skin. *IEEE Sens. J.* **1**, 41–51 (2001).
186. A. Schmitz, P. Maiolino, M. Maggiali, L. Natale, G. Cannata, G. Metta, Methods and technologies for the implementation of large-scale robot tactile sensors. *IEEE Trans. Robot.* **27**, 389–400 (2011).
187. P. Escobedo, M. Ntagios, D. Shakthivel, W. T. Navaraj, R. Dahiya, Energy generating electronic skin with intrinsic tactile sensing without touch sensors. *IEEE Trans. Robot.* **37**, 683–690 (2021).
188. R. S. Dahiya, G. Metta, M. Valle, G. Sandini, Tactile sensing—From humans to humanoids. *IEEE Trans. Robot.* **26**, 1–20 (2010).
189. M. D. Pickett, G. Medeiros-Ribeiro, R. S. Williams, A scalable neuristor built with Mott memristors. *Nat. Mater.* **12**, 114–117 (2013).
190. M. E. Beck, A. Shylendra, V. K. Sangwan, S. Guo, W. A. Gaviria Rojas, H. Yoo, H. Bergeron, K. Su, A. R. Trivedi, M. C. Hersam, Spiking neurons from tunable Gaussian heterojunction transistors. *Nat. Commun.* **11**, 1565 (2020).
191. K. Roy, A. Jaiswal, P. Panda, Towards spike-based machine intelligence with neuromorphic computing. *Nature* **575**, 607–617 (2019).
192. C. G. Núñez, W. T. Navaraj, E. O. Polat, R. Dahiya, Energy-autonomous, flexible, and transparent tactile skin. *Adv. Funct. Mater.* **27**, 1606287 (2017).
193. A. Vilouras, H. Heidari, S. Gupta, R. Dahiya, Modeling of CMOS devices and circuits on flexible ultrathin chips. *IEEE Trans. Electron Devices* **64**, 2038–2046 (2017).
194. M. Boniol, J.-P. Verriest, R. Pedeux, J.-F. Doré, Proportion of skin surface area of children and young adults from 2 to 18 years old. *J. Investig. Dermatol.* **128**, 461–464 (2008).
195. R. S. Johansson, A. B. Vallbo, Tactile sensibility in the human hand: Relative and absolute densities of four types of mechanoreceptive units in glabrous skin. *J. Physiol.* **286**, 283–300 (1979).
196. C. Yan, J. Wang, W. Kang, M. Cui, X. Wang, C. Y. Foo, K. J. Chee, P. S. Lee, Highly stretchable piezoresistive graphene–Nnanocellulose nanopaper for strain sensors. *Adv. Mater.* **26**, 2022–2027 (2014).
197. S. Luo, T. Liu, SWCNT/graphite nanoplatelet hybrid thin films for self-temperature-compensated, highly sensitive, and extensible piezoresistive sensors. *Adv. Mater.* **25**, 5650–5657 (2013).
198. S. Yao, Y. Zhu, Wearable multifunctional sensors using printed stretchable conductors made of silver nanowires. *Nanoscale* **6**, 2345–2352 (2014).
199. N. Lu, C. Lu, S. Yang, J. Rogers, Highly sensitive skin-mountable strain gauges based entirely on elastomers. *Adv. Funct. Mater.* **22**, 4044–4050 (2012).
200. M. Amjadi, Y. J. Yoon, I. Park, Ultra-stretchable and skin-mountable strain sensors using carbon nanotubes–Ecoflex nanocomposites. *Nanotechnology* **26**, 375501 (2015).
201. J. Choi, K. Hong, 3D skin length deformation of lower body during knee joint flexion for the practical application of functional sportswear. *Appl. Ergon.* **48**, 186–201 (2015).
202. G. Corniani, H. P. Saal, Tactile innervation densities across the whole body. *J. Neurophysiol.* **124**, 1229–1240 (2020).
203. B. Ibrahim, J. McMurray, R. Jafari, A wrist-worn strap with an array of electrodes for robust physiological sensing, in *2018 40th Annual International Conference of the IEEE Engineering in Medicine and Biology Society (EMBC)* (IEEE, 2018), pp. 4313–4317.
204. F. Mancin, Whole-body mapping of spatial acuity for pain and touch. *Ann. Neurol.* **75**, 917–924 (2014).
205. Y. Jiang, P. Huang, D. Zhu, Z. Zhou, R. Han, L. Liu, X. Liu, J. Kang, Design and hardware implementation of neuromorphic systems with RRAM synapses and threshold-controlled neurons for pattern recognition. *IEEE Trans. Circuits Syst. I Regul. Pap.* **65**, 2726–2738 (2018).
206. P. M. Sheridan, F. Cai, C. du, W. Ma, Z. Zhang, W. D. Lu, Sparse coding with memristor networks. *Nat. Nanotechnol.* **12**, 784–789 (2017).

Funding: This work was supported by Engineering and Physical Sciences Research Council (EPSRC) through Engineering Fellowship for Growth - neuPRINTSKIN (EP/R029644/1) and Hetero-print Programme Grant (EP/R03480X/1). **Author contributions:** R.D., Y.S., and M.K. conceptualized the review. F.L., S.D., A.C., and R.D. wrote the manuscript. R.D., Y.S., and M.K. guided the topics of discussion and structure of the review. All authors provided feedback and revisions. R.D. provided overall supervision of the work. **Competing interests:** The authors declare that they have no competing interests.

Submitted 2 August 2021
Accepted 13 May 2022
Published 8 June 2022
10.1126/scirobotics.abl7344

Downloaded from https://www.science.org at Huazhong University of Science and Technology on September 02, 2026

Science Robotics

Neuro-inspired electronic skin for robots

Fengyuan Liu, Sweety Deswal, Adamos Christou, Yulia Sandamirskaya, Mohsen Kaboli, and Ravinder Dahiya

Sci. Robot. **7** (67), eabl7344. DOI: 10.1126/scirobotics.abl7344

View the article online
https://www.science.org/doi/10.1126/scirobotics.abl7344
Permissions
https://www.science.org/help/reprints-and-permissions

Downloaded from https://www.science.org at Huazhong University of Science and Technology on September 02, 2026

Use of this article is subject to the Terms of service

Science Robotics (ISSN 2470-9476) is published by the American Association for the Advancement of Science. 1200 New York Avenue NW, Washington, DC 20005. The title *Science Robotics* is a registered trademark of AAAS.

Copyright © 2022 The Authors, some rights reserved; exclusive licensee American Association for the Advancement of Science. No claim to original U.S. Government Works